The connectivity of the brain: multi-level quantitative analysis

J.M.J. Murre and D.P.F. Sturdy
Medical Research Council - Applied Psychology Unit[1]

Abstract

We develop a mathematical formalism for calculating connectivity volumes generated by specific topologies with various physical packing strategies. We consider four topologies (full, random, nearest neighbor, and modular connectivity) and three physical models: *(i)* interior packing, where neurons and connection fibers are intermixed, *(ii)* sheeted packing where neurons are located on a sheet with fibers running underneath, and *(iii)* exterior packing where the neurons are located at the surfaces of a cube or sphere with fibers taking up the internal volume. By extensive cross-referencing of available human neuroanatomical data we produce a consistent set of parameters for the whole brain, the cerebral cortex, and the cerebellar cortex. By comparing these inferred values with those predicted by the expressions, we draw the following general conclusions for the human brain, cortex, cerebellum: *(i)* Interior packing is less efficient than exterior packing (in a sphere). *(ii)* Fully and randomly connected topologies are extremely inefficient. More specifically we find evidence that different topologies and physical packing strategies might be used at different scales. *(iii)* For the human brain at a macrostructural level, modular topologies on an exterior sphere approach the data most closely. *(iv)* On a mesostructural level, laminarization and columnarization are evidence of the superior efficiency of organizing the wiring as sheets. *(v)* Within sheets, microstructures emerge in which interior models are shown to be the most efficient. With regard to interspecies similarities and differences we conjecture *(vi)* that the remarkable constancy of number of neurons per underlying mm^2 of cortex may be the result of evolution minimizing interneuron distance in grey matter, and *(vii)* that the topologies that best fit the human brain data should not be assumed to apply to other mammals, such as the mouse for which we show that a random topology may be feasible for the cortex.

1. Introduction

Given fundamental constraints on the size of the skull, what are the factors that determine the structure of the brain? By structure we mean, for example, the existence of covering sheets of neurons in cortices, the modularity and laminarity of cortex, and intriguing

[1] The authors can now be reached at: J.M.J. Murre, University of Amsterdam, Psychonomics, Roetersstraat 15, 1018 WB Amsterdam, The Netherlands. E-mail: pn_murre@macmail.psy.uva.nl. D.P.F. Sturdy, CB1 Computer Cafe, 32 Mill Road, Cambridge CB1 2AD, UK. E-mail: sturdy@cb1.com. We thank Graeme Mitchison and one anonymous reviewer for their helpful comments. This work was supported by the Medical Research Council.

constancies such as the constant number of neurons per mm^2 (Bok, 1959; Braitenberg and Schüz, 1991; Rockel, Hiorns, and Powell, 1980). In this paper, we present an initial attempt to investigate some of the major constraints on the structure of the brain. In order to do this we draw heavily on existing quantitative neuroanatomical data. We have found rich databases at the microscopic and macroscopic levels. Neither of these gives immediate answers to our questions, which require anatomical data at an intermediate level. Such data have to be inferred, a process which has been reported to produce startling inconsistencies (Cherniak, 1990). The existence of these great inconsistencies is our main reason for drawing attention to this level by calling it the 'mesostructure'. Another reason is that the development of realistic computational simulations requires a solid database from which to work. Connectionist models are now reaching the stage where they are used to model large-scale neuroanatomical structures such as the hippocampus (e.g., Rolls, 1990). Progress in this area is crucially dependent on the production of accurate mesostructural figures.

We have chosen a mathematical approach to make structural inferences in an explicit and systematic manner. Our primary assumption in this work is that the brain aims to maximize connectivity while minimizing volume (cf. Cherniak, 1994; Mitchison, 1991, 1992). We study several topologies (connectivity patterns) within various physical models, both of the whole brain and of parts of the brain.

The topology is an abstract structure (technically, it would be a graph of neurons with interconnections). To derive its physical characteristics we must position it in space. There are several models we can use for positioning the neurons in the brain: we analyze the 'interior model' and the 'exterior cube model', which we subsequently refine to the 'exterior sphere model'. In the interior model, neurons are positioned equidistantly in three dimensions with connections running between neurons; the shape of such a model does not matter for the resulting volumes. In the exterior cube model, neurons are positioned equidistantly in two dimensions in sheets located on the surface of the cube, with connecting structures running through its internal volume.

Our analyses provide a set of parameterized expressions for the volume of the brain. To assess their plausibility we need reliable estimates for these parameters. Few of these estimates are well established, others need to be inferred often from figures which have very large variability. Our inferences rely on extensive cross-referencing between the microscopic and macroscopic levels, the kind of neuroanatomical 'bean counting' referred to by Cherniak (1990).

Recent studies (e.g., Abeles, 1991; Braitenberg and Schüz, 1991; Shepherd, 1974; White, 1989) have furthered our insights into microscopic connectivity, within the millimeter range. On a macroscopic level, Felleman and Van Essen (1991), for example, give the overall connectivity pattern for all known areas of the visual system.

On an intermediate level, however, very little is known about connectivity patterns in general. It is possible to trace the main target areas of a given area by several techniques, but the question of how many long-range connections a single neuron makes is very difficult to investigate with any of the current methods, because this involves identifying up to 10,000 post-synaptic neurons that can be located anywhere in the brain. For certain areas, such as the hippocampus (Seifert, 1984; Treves and Rolls, 1994) and the basal forebrain (Mesulam *et al.*, 1983), the mesoanatomy is known in great detail, but for others such as the cerebral cortex much remains unknown. We propose to infer the mesoanatomy of certain areas in the brain by combining anatomical quantities at a microscopic level (e.g., neuron volume, axon radius) with macroscopic quantities (e.g.,

brain volume). We will investigate the plausibility of several connectivity patterns, starting with the admittedly implausible hypothesis that the brain is wired regularly, and then trying to refine these approximations.

Neural network models often assume full-connectivity between an input and an output layer (Kosko 1987, 1988; Steinbuch, 1961; Anderson, 1972; Kohonen, 1972; and Nakano, 1972), possibly involving one or more 'hidden layers' (Ackley, Hinton, and Sejnowski, 1985; Rumelhart, Hinton, and Williams, 1986). Some network models assume full, bidirectional (or recurrent) connectivity between all their nodes (Hopfield, 1982, 1984). Most researchers admit that full connectivity is not a plausible topology for the brain. Many studies have, therefore, investigated sparse, random connectivity patterns (e.g., Anninos *et al.*, 1970; Derrida, Gardner, and Zippelius, 1987; Harth *et al.*, 1970; Nelken, 1988; Shinomoto, 1987), assuming that this is a more plausible model of the brain. In these networks, a given node is connected to a random fraction of the available nodes. Another popular connectivity pattern is the topological map (e.g., Kohonen, 1989, 1990). In these maps, the most active node wins a competition process and both its own weights and those of its neighbors are updated during the training phase. Though in most implementations any given node must communicate its activation value to all other nodes to derive the 'winner', the underlying theoretical model assumes only local connectivity of the 'nearest-neighbors' type. A fourth type of connectivity is a modular topology (e.g., Grossberg, 1976, 1982, 1987; Murre, 1992, 1993). These networks consist of many modules. Connectivity within a module may be dense, but any given module is connected to only a small subset of the available modules. There is mounting consensus that this type of connectivity pattern is both the most plausible and the most practical.

2. Method of analysis

We consider four topologies or connectivity patterns: *(1)* full connectivity, *(2)* random (sparse) connectivity, *(3)* modular connectivity, and *(4)* nearest neighbor connectivity. The effect of these topologies on volume is studied in two contrasting models of the brain: the interior and exterior models. In this section, we present the derivation of the expressions for brain volume. A brief summary is provided at the end of this section in Table 2. In Section 3, we use these results to investigate the plausibility of the different topologies and models. Table 1 presents a complete listing of all the symbols used in this paper.

2.1 Analyses with the interior model

In this model we assume that there are n neurons, positioned inside a 3-dimensional structure, for example, a cube or a sphere. The derivations below apply equally to both, as well as to most other shapes. This distribution can be contrasted with that where the neurons are located in a limited number of very dense clusters. This case is not as relevant for biological brains and will therefore not be considered here, but it has been analyzed in some detail by Murre (1993) for neural network implementations on multi-processor hardware. Interneuron distance x is the same in all three directions. We assume that neuron bodies themselves do not occupy any space (in actual fact, they take up about 3%

A	total axon (fiber) volume (in m^3)
a	single axon (fiber) volume (in m^3)
b	intermodular branching factor
C	constant used in the exterior radius and volume expressions
F	connectivity factor in modular topologies ($F = m/n$)
f	connectivity factor in random topologies ($f = 1$ is full connectivity)
h	distance between target neurons (in m)
k	number of nearest neighbors
m	number of modules
n	number of neurons
r	axon radius (in m)
R	brain radius for the sphere model (in m)
s	cross-sectional axon surface area ($s = \pi r^2$ in m^2)
V	brain volume (in m^3)
x	distance between neurons (in m)

The symbols may carry a subscript emphasizing the model or type of connectivity of the network topology:

full	full
ran	random
mod	modular
near	nearest neighbors

Table 1. Complete list of all symbols used with their meanings. We use the $O(.)$ notation in its familiar meaning, in this paper indicating the highest power of a polynomial function (e.g., $O(n^2)$ indicates a quadratic increase with n, ignoring constants and lower powers).

of the brain, see Table 3). We combine the volume of dendrites with that of axons, which thus stand for connection structures (fibers) in general. We also ignore the supporting structures (e.g., glial cells, blood vessels, etc.) and concentrate purely on the connection volume A of the various topologies.

In all derivations we assume that an axon 'snakes' along all its target neurons as, for example, the parallel fibers which snake along Purkinje cells in cerebellum. Both axons and dendrites often exhibit elaborate arborization, but arborization does not in itself reduce total axon length. In particular, any branching structure in a two- or three-dimensional lattice, in which the branching points coincide with the neurons, can be replaced by a 'snaking' structure that has the same total path length (see Figure 1). Following Mitchison (1991), we assume that the cross-sectional area (or radius r) of an axon remains constant. Derivations based on snaking axons are more straightforward, which is why we use them here. We emphasize that in all cases a snaking axon can be replaced by a branching one, and that there is thus no loss of generality in using the snake model.

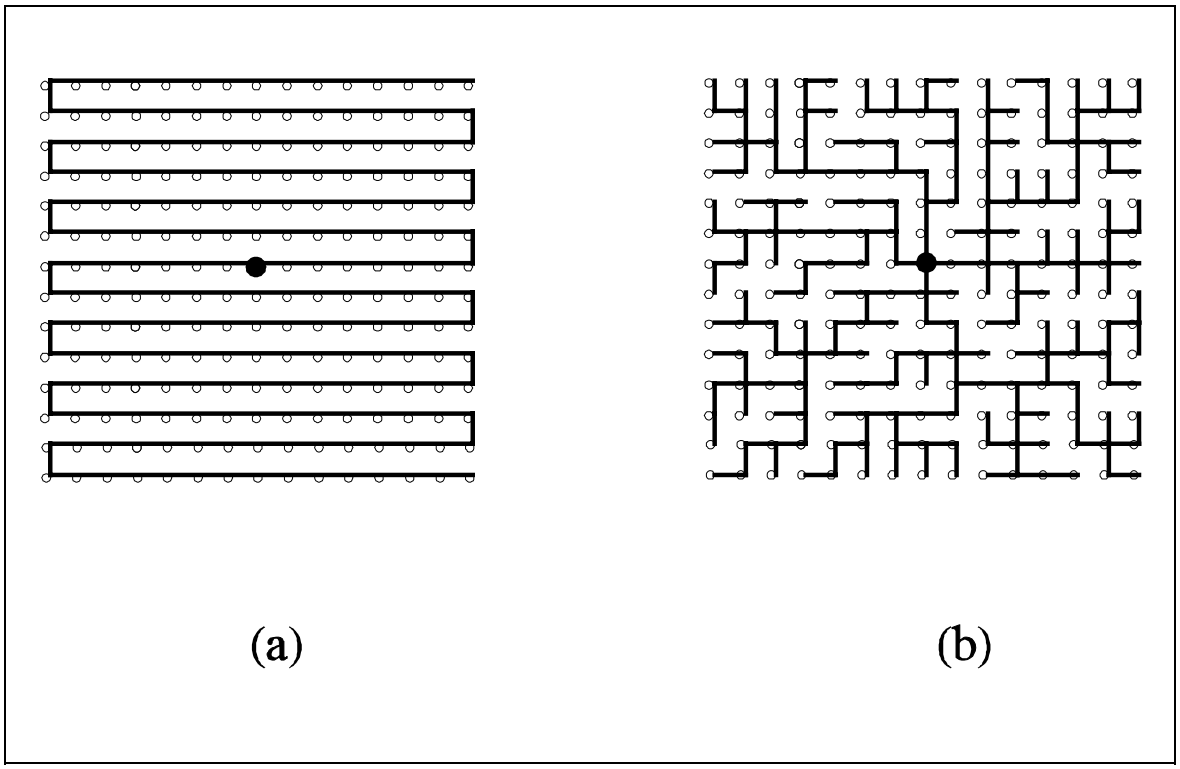

Figure 1. Two connection strategies. A pre-synaptic neuron (black circle) connects to 209 post-synaptic neurons (white circles). (a) A snaking connection strategy. (b) A branching connection strategy. Total fiber length is equal in (a) and (b), but longest path length in (b) is $O(\sqrt{n})$, whereas longest path length is $O(n)$ in (a). It is impossible for this example to find a shorter path length using branching.

The proposed connection strategy of 'snaking' is optimal under the above assumptions (i.e., rectangular grid, branching points coincide with neurons). With a snaking axon each neuron connects to at least one other neuron. If the neurons are a distance x apart, then with n neurons the axon will be of length nx (actually $(n\text{-}1)x$, because the last neuron does not need to connect to any others; we ignore the effect of the last segment). No snaking structure can be shorter because it would either have less than n elements or segments that were shorter than x, both of which are impossible.

The same argument applies to a branching structure. This must also connect to all n neurons and each neuron must, therefore, receive at least one incoming connection. This gives a total of n incoming connections, each of which is at least length x, because this is the shortest possible distance between any two grid points. Hence, any branching structure is at least of length nx, and is thus not more effective than the snake model. If we allow internal branching points, we can devise connection schemes that are more efficient than a snaking model, but the gain is small. In these more complicated models total axon length still scales linearly with n and using such a model will not affect the order of our

approximations. Finally, when neurons are not distributed neatly in a lattice, additional reductions in path-length may be obtained by optimization strategies. The resulting problem is a Traveling Salesman Problem, which is well known to be NP-complete. This rules out the possibility of neurons actually finding optimal solutions to this problem. Suboptimal solutions may still result in shorter path lengths than a snaking neuron, but again we expect this effect to be small. A large effect is only to be expected if the neurons are distributed in clusters with small within-cluster distances and large between-cluster distances. This topology, however, is treated separately in this paper.

2.1.1 Full connectivity (interior)

The volume for a single axon can be derived immediately by simply multiplying the number of neurons n to which it must connect with interneuron distance x and with the axon's cross-sectional surface $s=\pi r^2$:

$$a = \pi r^2 x n = s x n \tag{1}$$

Thus the sum of all axon volumes is

$$A = a n = \pi r^2 x n^2 = s x n^2 \tag{2}$$

We can find x by equating A with nx^3, which is the expression for the total volume of the cube: n little cubes of volume x^3:

$$x^3 n = \pi r^2 x n^2 \tag{3}$$

Thus

$$x = r\sqrt{\pi n} \tag{4}$$

so that the total volume with full connectivity becomes

$$V_{full} = x^3 n = \pi^{\frac{3}{2}} r^3 n^{\frac{5}{2}} = s^{\frac{3}{2}} n^{\frac{5}{2}} \tag{5}$$

Thus, increasing the number of neurons leads to almost a cubic increase in the volume of the brain. For instance, if the number of neurons in a one-liter brain is tripled, its volume would increase to more than 15 liters.

2.1.2 Random connectivity (interior)

We use the same model and parameters as above, but now any given neuron is connected to only a fraction f of the neurons, with $0 < f < 1$. We call f the connectivity factor. With random-connectivity topologies it is unfeasible to determine the shortest connecting path. A simplifying assumption is that the post-synaptic (target) neurons are distributed regularly throughout the brain. This stratification assumption makes it a quasi-random connectivity. This will influence the precise relationships derived, but not significantly. If the target

neurons are spread regularly throughout the cube, they will be spaced nearly equidistantly. As above a neuron's axon snakes along all its target neurons. Target neurons are *h* meters apart, with

$$h = \frac{n^{\frac{1}{3}}}{(fn)^{\frac{1}{3}}} x = f^{-\frac{1}{3}} x \qquad \textbf{(6)}$$

So, with $f = 10^{-6}$ and $h = 100x$ m, about 100 neurons would lie in between two target neurons. Target neurons can be visualized as lying inside 'large cubes' with sides *h*. Since the axon no longer snakes along all neurons, but only along the centers of the 'large cubes', the length of each axon is shortened considerably.

Under the above assumptions we derive for a random-connectivity topology the following expressions for single axon volume *a* and total axon volume *A*:

$$a = \pi r^2 hfn = \pi r^2 f^{-\frac{1}{3}} xfn = \pi r^2 f^{\frac{2}{3}} xn \qquad \textbf{(7)}$$

and

$$A = an = \pi r^2 f^{\frac{2}{3}} xn^2 \qquad \textbf{(8)}$$

As above, we equate *A* with nx^3 to derive an expression for *x*:

$$x^3 n = \pi r^2 f^{\frac{2}{3}} xn^2 \qquad \textbf{(9)}$$

$$x = \sqrt{\pi n} rf^{\frac{1}{3}} \qquad \textbf{(10)}$$

This results in a total volume

$$V_{ran} = \pi^{\frac{3}{2}} n^{\frac{5}{2}} r^3 f = s^{\frac{3}{2}} n^{\frac{5}{2}} f \qquad \textbf{(11)}$$

where *s* is as above. Reductions in connectivity have a linear effect on brain volume: $V_{ran} = V_{full} f$.

2.1.3 *k*-Nearest neighbor connectivity (interior)

Each neuron is connected to *k* nearest neighbors. Under the present assumptions, whereby an axon snakes along the post-synaptic targets, the neurons do not need to be the nearest ones in some metric sense. It is sufficient that they form a contiguous chain that includes the pre-synaptic neuron. So, the *k*-nearest neighbor topology includes one-dimensional, two-dimensional and three-dimensional maps as special cases. Derivation of the volume

expressions for this topology is straightforward. Each neuron is connected to *k* neurons in the neighborhood. Thus the single axon volume *a* is *sxk* and the total axon volume is

$$A = nsxk \tag{12}$$

We equate this with nx^3, as for the other topologies:

$$x = (sk)^{\frac{1}{2}} \tag{13}$$

and

$$V_{near} = n(sk)^{\frac{3}{2}} \tag{14}$$

Volume scales linearly with *n*, but increasing *k* has a more than linear effect.

2.1.4 Modular connectivity (interior)

By dividing the network into a number of modules and thereby limiting the number of long-range targets, connection length is reduced. Within-module connections may be dense, but connectivity at the module level is sparse: each module is connected to only a small subset of the available modules (Murre, 1992, 1993). There is a long tradition of modular models of the brain (e.g., Mountcastle, 1978; Szenthágothai, 1975). Most of these models imply that neurons within a given module send axons to the same target modules. This particular constraint, however, has no effect on brain volume and we will therefore use a slightly more general approach that allows neurons within one module to have different targets.

Modularity is defined with respect to the branching pattern of individual neurons, as follows: *(i)* A single neuron sends an long-range axon to a constant number *m* of remote sites (modules), randomly distributed throughout the brain. *(ii)* There is extensive short-range, local branching in a target module to an average *b* post-synaptic neurons. We ignore the variance in *b* and treat it as a constant. As explained above, it is not necessary to define modules a priori. Any branching pattern that conforms to this definition will be called modular. Part *(i)* of the definition is equal to that of random connectivity, except that we are here using a fixed connectivity by setting *m* constant (i.e., independent of *n*). Part *(ii)* is of a *k*-near type.

We use the same approach as above for the derivation of volume expressions for modular topologies, assuming the approximate equidistance of randomly distributed modules. Axon volume can be decomposed into global axon volume A_g, consisting of long-range axons, and local axon volume A_l, consisting of short-range within-module branching. The modules are again located in *m* 'large cubes' each cube containing *n*/*m* neurons. This gives intermodule distances of $(n/m)^{1/3}x$ m. Each of *n* neurons sends an axon to *m* such cubes, so that the total global axon volume is

$$A_g = nmsxn^{\frac{1}{3}}m^{-\frac{1}{3}} = sxn^{\frac{4}{3}}m^{\frac{2}{3}} \tag{15}$$

where $s = \pi r^2$ is again the cross-sectional axon surface. Local branching contributes *bxm* to each of *n* neurons, so total local axon volume is

$$A_l = nmsbx \tag{16}$$

Total volume is $V_{mod} = A_g + A_l = nx^3$, from which we can derive *x*:

$$nx^3 = sxn^{\frac{4}{3}}m^{\frac{2}{3}} + nmsbx \tag{17}$$

$$x = \left(sn^{\frac{1}{3}}m^{\frac{2}{3}} + smb\right)^{\frac{1}{2}} \tag{18}$$

and

$$V_{\text{mod}} = nx^3 = n\left(sn^{\frac{1}{3}}m^{\frac{2}{3}} + smb\right)^{\frac{3}{2}} = s^{\frac{3}{2}}n^{\frac{3}{2}}\left(m^{\frac{2}{3}} + n^{-\frac{1}{3}}mb\right)^{\frac{3}{2}} \tag{19}$$

For relatively small constant-size modules, *mb* can be ignored and for large *n*, we have

$$V_{\text{mod}} \approx s^{\frac{3}{2}}n^{\frac{3}{2}}m = V_{full}\frac{m}{n} = V_{full}F \tag{20}$$

Where $F = m/n$. Volume scales $O(n^{3/2})$ instead of $O(n^{5/2})$ as in the case of full or random connectivity. The number of modules *m* in this analysis is taken as constant, but as explained above this applies only to a single neuron. That is, a single neuron can synapse to a fixed number of modules, no matter what the size of the brain, but the total number of modules in the brain is not restricted. If the number of neurons doubles, the number of modules might - but need not - double as well.

A major difference with the random topology is that the connections from a neuron are restricted to a constant number *mb* of target neurons. In the random topology we allowed the number of connections to vary with *n* by setting the number of target neurons to *fn*. In the extreme case where the modules are all of size one, we have in effect a non-modularized random topology. In that case we have $V_{mod} \approx V_{ran}$.

2.2 Analyses with the exterior cube model

In the exterior cube model, all the neurons are placed in sheets on the six surfaces of the cube. This approximates to the grey matter in the brain, with connecting structure filling the internal volume, the white matter. In order to derive the expressions for this model, we firstly look at one sheet as a single surface.

The sheet model assumes that all neurons are located at the top of a single square two-dimensional sheet with the axons running in a volume below this sheet. As with the interior model, we assume that the neuron soma volume itself does not contribute

significantly to the total brain volume. A major difference with the interior model is that we can now derive the brain volume for any preset interneuron distance, *x*, rather than having *x* determined by the number of neurons, axon radius and connectivity factor. As with the interior model, we use the wiring strategy whereby a non-branching axon snakes along all post-synaptic neurons, which are again spaced equidistantly.

2.2.1 Full connectivity (sheet)

The expression for single axon volume *a* is straightforward. A neuron connects to *n* neurons which are *x* meters apart. This gives an axon length of *xn*, a volume

$$a = \pi r^2 x n \tag{21}$$

and a total axon volume

$$A = \pi r^2 x n^2 = s x n^2 \tag{22}$$

where $s = \pi r^2$ is the cross-sectional axon surface. For the sheet model, the axon volume *A* immediately gives the brain volume V_{full}. We see that increasing *x* gives a linear increase in total brain volume *V*.

2.2.2 Random connectivity (sheet)

As with the interior model we assume that each neuron is connected to *fn* neurons, quasi-randomly distributed on the sheet. Each target neuron lies in the center of a large square. There are *fn* such squares, each with about $n/fn = f^{-1}$ neurons. This results in a length of $f^{-½}$ neurons for the side of a large square. The interneuron distance is fixed at *x* meters, and the number of target neurons is *fn*. Multiplying these numbers with the axon surface *s* gives the single axon volume

$$a = s x n f^{\frac{1}{2}} \tag{23}$$

and the total volume

$$V_{ran} = s x n^2 f^{\frac{1}{2}} \tag{24}$$

Compared with the interior model reducing connectivity has a much smaller effect in a sheet. For example, reducing connectivity by a factor 100 would produce a hundredfold decrease in (interior) brain volume, but only a tenfold decrease in sheet brain volume (also see Mitchison, 1992).

2.2.3 *k*-Nearest neighbor connectivity (sheet)

If a neuron is connected to *k* others, axon length is *kx*, axon volume is

$$a = sxk \tag{25}$$

and total volume is

$$V_{near} = sxkn \tag{26}$$

We see that volume scales linearly with k and with n.

2.2.4 Modular connectivity (sheet)

We use the same definition for modularity as for the interior model, where a neuron connects to $m = Fn$ modules, $0 < m < n$, distributed quasi-randomly throughout the sheet with local branching to b neurons in each module. We distinguish two contributions to axon volume: *(i)* Volume A_g, global or long-range connections to the different modules, and *(ii)* volume A_l, local, within module branching.

As before, we assume that the long-range axon snakes along the center of all large squares in which the modules are located. There are m such squares, each with length $F^{-½}$. The derivation for A_g is fully analogous to that of V_{ran}

$$A_g = sxn^2F^{\frac{1}{2}} \tag{27}$$

The contribution of local branching to single axon length in a single module is simply bx, and mbx for all modules: $a_l = sxmb$, $A_l = na_l$. This gives the following expression for $V_{mod} = A_g + A_l$

$$V_{\mathrm{mod}} = sxn^2F^{\frac{1}{2}} + sxnmb \tag{28}$$

$$= sxn^2\left(\frac{m}{n}\right)^{\frac{1}{2}} + sxnmb \tag{29}$$

$$= sx(n^{\frac{3}{2}}m^{\frac{1}{2}} + nmb) \tag{30}$$

where we have substituted m/n for $F^{-½}$. As is to be expected, the effect of long-range connections is strongly influenced by the number of modules. The extent of local branching has a linear effect.

2.2.5 Exterior cube model

We now use the above expressions to derive exterior cube volumes. The surface area of a cube with radius R is $24R^2$, where R is half the edge length. We use radius R rather than diameter to simplify refinement of this model to a sphere variant. There are n neurons,

spaced equidistantly on the surface of the cube, each occupying a small square of $24R^2/n$. By taking the square root of this we obtain an expression for x:

$$x = \sqrt{24} n^{-\frac{1}{2}} R \tag{31}$$

We use the formula for the total axon volume of a fully connected brain on the sheet, sxn^2, and equate that with the volume of the cube, substituting the derived value for x.

$$sxn^2 = s\sqrt{24} n^{-\frac{1}{2}} Rn^2 = 8R^3 \tag{32}$$

$$R^2 = \frac{\sqrt{24}\pi}{8} r n^{\frac{3}{2}} \tag{33}$$

$$R = C_c r n^{\frac{3}{4}} \tag{34}$$

where C_c is a constant for the exterior cube:

$$C_c = \left(\frac{\sqrt{24}\pi}{8} \right)^{\frac{1}{2}} \approx 1.387 \tag{35}$$

This results in a volume of

$$V_{full} = 8C_c^3 r^3 n^{\frac{9}{4}} \approx 21.35 r^3 n^{\frac{9}{4}} \tag{36}$$

In a similar way we derive expressions for the radius R in the random, k-near, and modular topologies:

$$R_{ran} = C_c r n^{\frac{3}{4}} f^{\frac{1}{4}} \tag{37}$$

$$R_{near} = C_c r k^{\frac{1}{2}} n^{\frac{1}{4}} \tag{38}$$

$$R_{\mathrm{mod}} = C_c r n^{\frac{1}{2}} (m^{\frac{1}{2}} + n^{-\frac{1}{2}} mb)^{\frac{1}{2}} \tag{39}$$

2.2.6 The exterior sphere model

We introduce here a slight refinement to the exterior cube model: the exterior sphere model, first used by Nelson and Bower (1990). This physical model assumes that all neurons are located on the surface of a sphere, the axons running through its volume. With a fully connected topology, and with $n = 10^{11}$ and $r = 10^{-7}$, they calculated that such a sphere would need a diameter of 10 km to accommodate the volume taken up by the axons. They do not describe how they arrived at their estimate. In the light of our findings they must have used extremely unfavorable assumptions about routing (e.g., a separate axon to each neuron). In our version of the sphere model, we also assume that all neurons are distributed equidistantly on the surface of a sphere with the axons running through its volume, but we use a sheet model for the physical realization of connectivity. This is fully analogous to the exterior cube model.

The sphere model appears to be a good approximate model for the brain, for example when considering the grey matter and white matter of the cortex. In the latter case, however, we must keep in mind that the cortex is strongly folded. Thus, the total surface area of the cortex of 0.1658 m^2 (see below) implies a virtual radius of 23.0 cm. That is, if we unfold the cortex, its radius would increase to almost half a meter in diameter, rather than its present diameter of about 14 cm. Of course, these values are only valid if the cortex were indeed a folded sphere. Though we know that this is not the case (e.g., Jouandet *et al*., 1989), it is still interesting to consider this model because it has the lowest volume/surface ratio and thus forms an optimal case. Furthermore, in other animals, for example the mouse, the cortex does in fact approach an ellipsoid in so far as it is completely devoid of folds.

As it turns out, the volume expressions for the exterior cube model are exactly the same as for the exterior sphere model, except that the constant is different for the sphere (also see Table 2 below), namely

$$C_s = \left(\frac{3}{2}\right)^{\frac{3}{2}} \pi^{\frac{3}{4}} r^3 \approx 4.335 \times 10^{-21} \qquad \textbf{(40)}$$

All sphere volumes are five times smaller than the comparable cube volumes due to the fact that W_{sphere} is five times smaller than W_{cube}.

2.3 Discussion of the volume expressions

The twelve expressions that we have derived for connectivity volume in the brain are summarized in Table 2. The graphs in Figure 2 show the functions over various relevant parameter ranges. In these graphs the exterior cube model is used. Corresponding graphs for the exterior sphere model can be obtained by division of the ordinate values by a factor W_{sphere}/W_{cube} = 4.93. The brain parameters chosen here are illustrative only. In Section 3, we examine the neuroanatomical evidence to derive the actual values. Some conclusions to be drawn from these graphs are as follows:

Full connectivity. Figure 2a shows that the exterior model scales far more efficiently than the interior model, but that even for these very small numbers of neurons the connectivity volumes greatly exceed those of the brain.

Random connectivity. Figure 2b shows that both physical models scale in the same way with neuron number *n* for the very small - but realistic - value used for *f*. Examination of Table 2 reveals that in fact the random topologies scale in the same way as the full topologies, but this effect would only become evident for high *f* values or much larger *n*. This interaction between *f* and *n* is illustrated in Figure 2c, where for large *f* and *n* the two physical models diverge drastically. It is also clear that with anything but extremely small values for *f* the resulting volumes are very large, easily exceeding one cubic meter.

Neighbor connectivity. The *k*-nearest neighbor topology is shown in Figures 2d and 2e. For values of *k* up to half a million neighbors, volumes smaller than the brain are found for intermediate values of *n* (1-10 billion, i.e., 1-10 x 10^9). In Figure 2d a very large *k* of 5 million is used, revealing again the superior efficiency of the exterior model. This efficiency is also evident in Figure 2e, where an *n* of 1 billion for the interior model produces larger volumes than an *n* of 50 billion for the exterior cube model.

Modular connectivity. Figure 2f shows that both physical models scale similarly with *n*. But, as with the random topology illustrated in Figure 2b, this is only true for very low values of *m*. For very low numbers of modules the interior model is more efficient than the exterior cube model, but this effect reverses with large *m* as shown in Figure 2g. This is not true for the exterior sphere model where interior is always less efficient. For large *n*, intermodular branching *b* has little effect on the exterior model, but is a strong determinant of volume in the interior model.

Topology	**Neural packing model**		
	Interior	**Exterior**	**Sheet**
Full	$Sn^{\frac{5}{2}}$	$Wn^{\frac{9}{4}}$	Xn^2
Random	$Sn^{\frac{5}{2}}f$	$Wn^{\frac{9}{4}}f^{\frac{3}{4}}$	$Xn^2f^{\frac{1}{2}}$
***k*-Near**	$Snk^{\frac{3}{2}}$	$Wn^{\frac{3}{4}}k^{\frac{3}{2}}$	Xnk
Modular	$Sn^{\frac{3}{2}}\left(m^{\frac{2}{3}}+n^{-\frac{1}{3}}mb\right)^{\frac{3}{2}}$	$Wn^{\frac{3}{2}}\left(m^{\frac{1}{2}}+n^{-\frac{1}{2}}mb\right)^{\frac{3}{2}}$	$X(n^{\frac{3}{2}}m^{\frac{1}{2}}+nmb)$

Table 2. Expressions for brain volume under four topologies and three physical models. In the expressions, $S = \pi^{3/2}r^3 \approx 5.57 \times 10^{-21}$. For the exterior cube model $W = 8C_c{}^3r^3 \approx 2.14 \times 10^{-20}$, where $C_c = \left(\frac{\sqrt{24}\pi}{8}\right)^{\frac{1}{2}} \approx 1.387$. For the exterior sphere model $W = \left(\frac{3}{2}\right)^{\frac{3}{2}}\pi^{\frac{3}{4}}r^3 \approx 4.335\times10^{-21}$. For the sheet model $X = sx = \pi r^2 x \approx 1.41 \times 10^{-19}$.

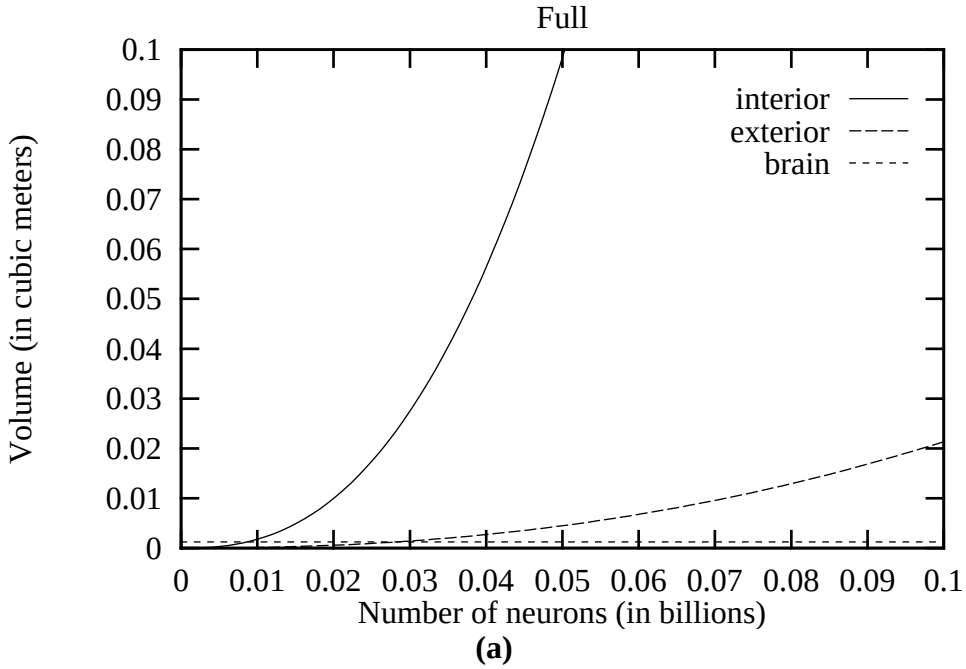
Full
Volume (in cubic meters)
Number of neurons (in billions)
interior
exterior
brain
0
0.01
0.02
0.03
0.04
0.05
0.06
0.07
0.08
0.09
0.1

(a)

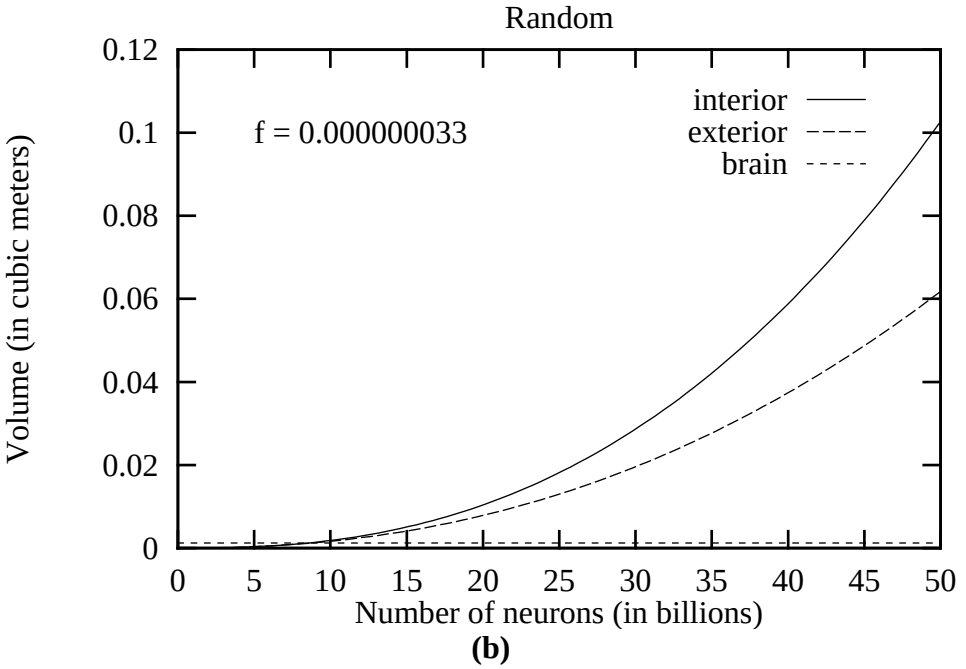
Random
Volume (in cubic meters)
Number of neurons (in billions)
f = 0.000000033
interior
exterior
brain
0
0.02
0.04
0.06
0.08
0.1
0.12
0
5
10
15
20
25
30
35
40
45
50

(b)

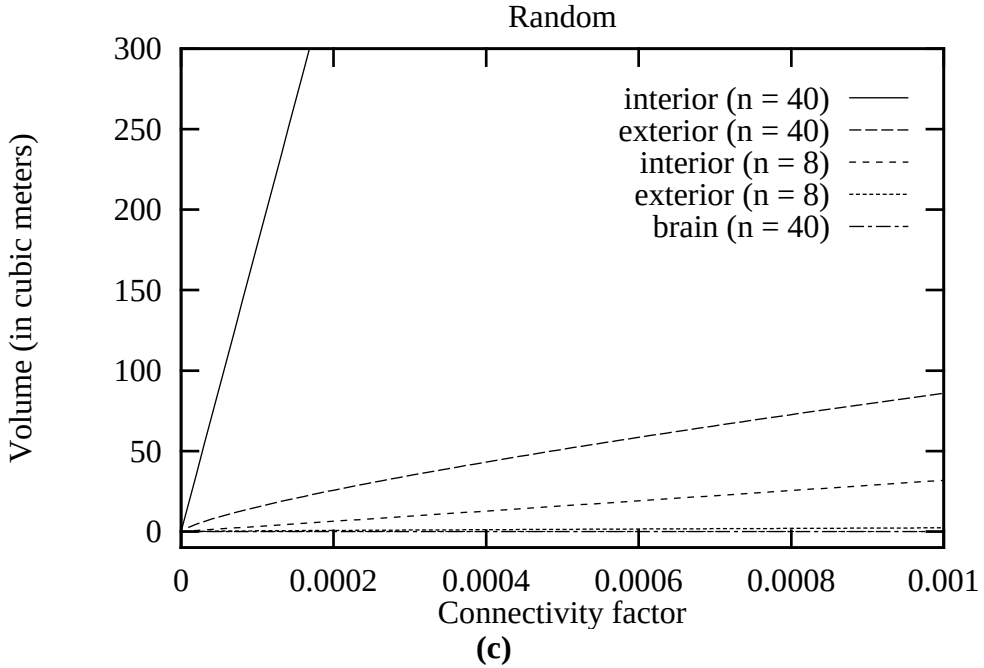
Random
Volume (in cubic meters)
Connectivity factor
interior (n = 40)
exterior (n = 40)
interior (n = 8)
exterior (n = 8)
brain (n = 40)
0
50
100
150
200
250
300
0
0.0002
0.0004
0.0006
0.0008
0.001

(c)

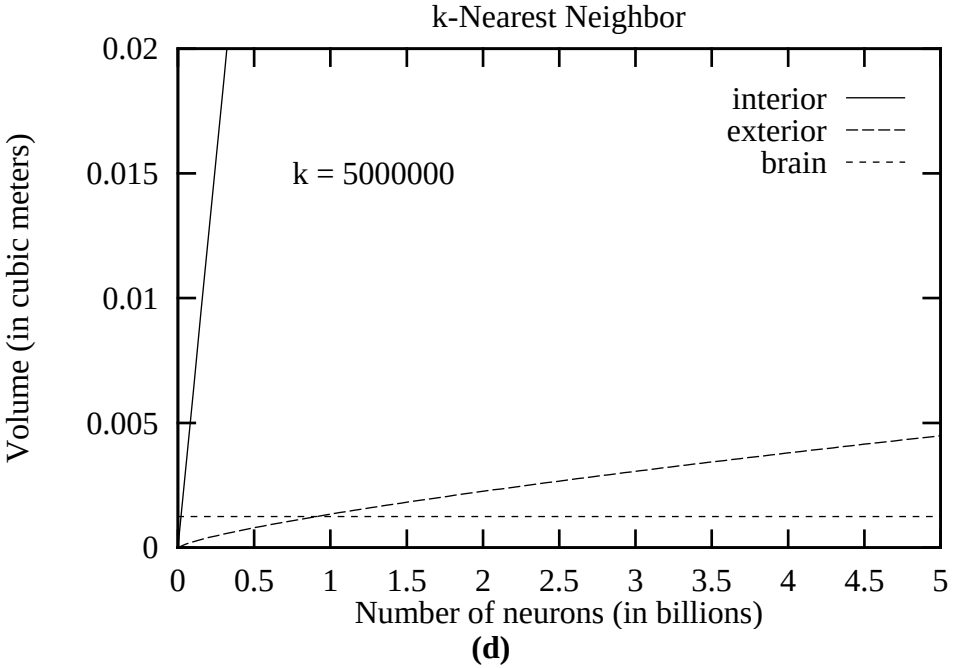
k-Nearest Neighbor
Volume (in cubic meters)
Number of neurons (in billions)
k = 5000000
interior
exterior
brain
0
0.005
0.01
0.015
0.02
0
0.5
1
1.5
2
2.5
3
3.5
4
4.5
5

(d)

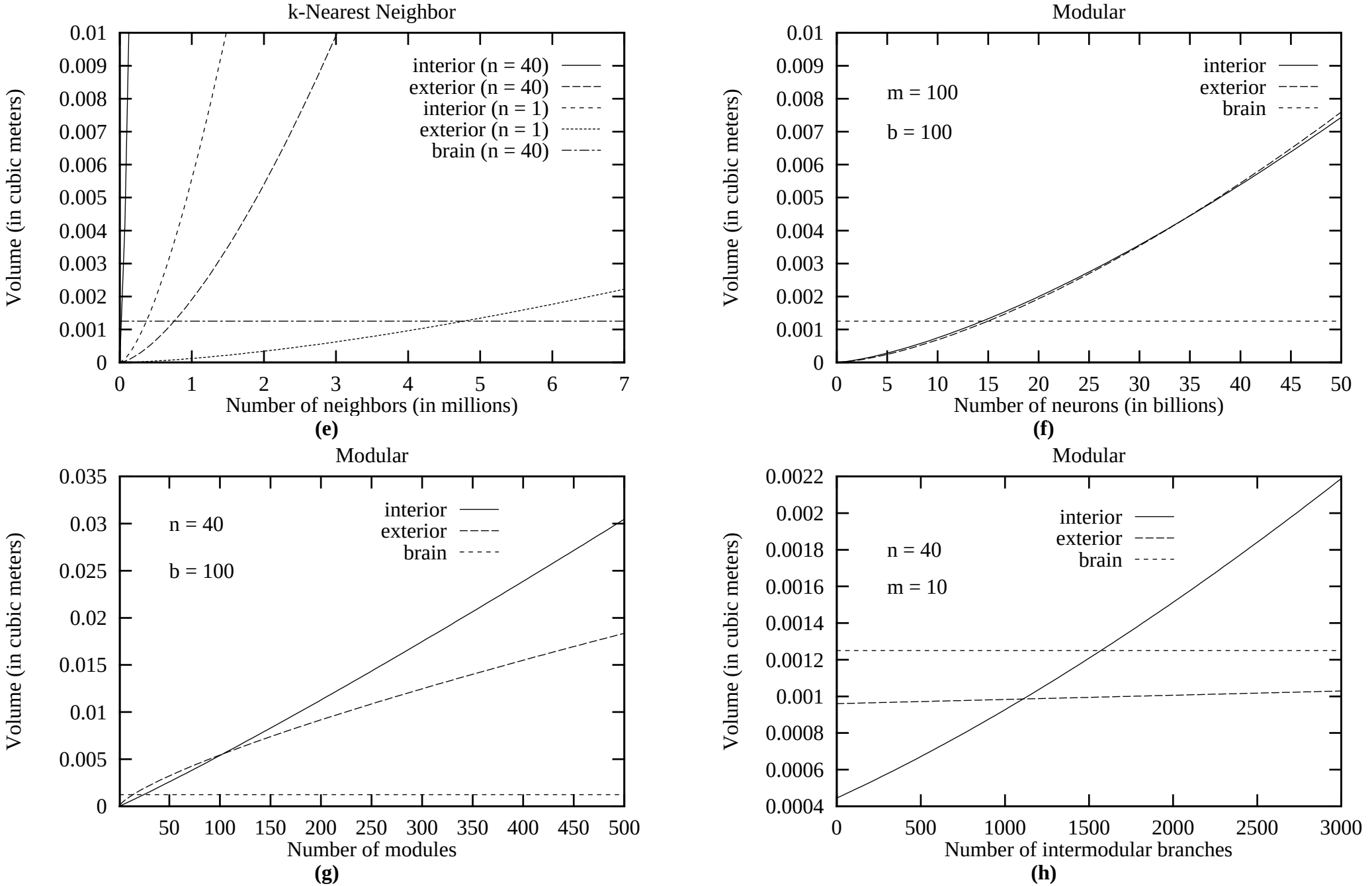

Figure 2. Comparison of volumes generated by the interior model and the exterior cube model. See text for explanation. The parameters used are r = 1.0 x 10^{-7} (or s = 3.14 x 10^{-14}) and x = 4.472 x 10^{-6}, and n is the number of neurons in billions (i.e., 10^9).

3. Application to neuroanatomical data

In this section we apply our method to the human brain by substituting the parameters in the expressions with known or inferred neuroanatomical values. Section 3.1 looks at the whole brain, considered as a homogeneous structure. Section 3.2 applies the same expressions to the figures available for the cortex, and section 3.3 briefly investigates the cerebellum. Each section is organized around two tables: one for the biological data and one for the results of applying the models to the data.

3.1 The homogeneous brain

Table 3 presents estimates for the human brain as a whole. In this section we consider as a first approximation the viewpoint that the brain is homogeneous. While we recognize that this not the case, it is nevertheless of interest to investigate the effect of different parameters on the brain as a whole. The principal reason why the brain is not homogeneous is that the cerebellum contains vast numbers of very small neurons. In Table 3, therefore, we present figures for the 'standard' or median neuron, irrespective of frequency, and for the 'average' or mean neuron, weighted for frequency.

The results of our first exploration are presented in Table 4. Most striking is the enormous volume of the fully connected brain in the interior cube model: a cube with a side of 121 m. Randomly limiting the connectivity results in a value that for all three physical models is much closer to the true brain volume. It is, however, still in the order of 30-300 times larger than the connectivity volume of the brain. This result strongly suggests that random models of the whole brain are not feasible.

For all physical models, a k-nearest neighbor topology gives very small connectivity volumes, implying that local branching up to a value of k = 10,000 adds little to the connectivity overhead.

The modular topology gives a volume that is still more than fifteen times too large for both for both interior and exterior cube (but with 10 times too many synapses). The exterior sphere model, however, produces a volume that is only three times too large. This result shows the value of modularity in reducing connectivity overhead in the brain.

All the results in this section should be treated merely as the first steps of an analysis. In particular the random topologies are heavily oversimplified in that they assume that the same low connectivity holds throughout the brain. In the next section we will, therefore, focus on one particular structure in the brain, namely the cortex. The homogeneity assumption seems to be more reasonable for this analysis (Braitenberg and Schüz, 1991; White, 1989).

Notes	Variable	Values	Percentage
1	brain volume	1252 cc	100%
1a	neuroglia	563 cc	45%
1b	neuron	376 cc	30%
1c	extracellular	250 cc	20%
1d	vascular	63 cc	5%
2	standard neuron volume	17200 μm^3	100%
2a	axon	1000 μm^3	6%
2b	dendrite	8500 μm^3	49%
2c	terminal	6000 μm^3	35%
2d	soma	1700 μm^3	10%
3	average neuron volume	9400 μm^3	100%
3a	axon	564 μm^3	6%
3b	dendrite	4606 μm^3	49%
3c	terminal	3290 μm^3	35%
3d	soma	940 μm^3	10%
4	number of neurons *(n)*	4×10^{10}	
5	total connection volume *(V=A)*	338 cc	
6	connectivity factor *(f)*	5.9×10^{-8}	
7	fiber radius *(r)*	0.1 µm	

Table 3. Estimated values of the independent variables for the human brain. Figures refer to the standard brain of standard man of weight 70 kg; standard woman is 10% smaller; figures have a variation of at least ±10%.

Notes to Table 3

1. Stephan et al. (1970): net volume, i.e., ventricles, meninges and nerves excluded.

1a. Cherniak (1990); 50% in Carpenter and Sutin (1983).

1b. Extrapolated from 35% for rat cortex (Vernadakis, 1986) and 35-40% for human neocortex (Pope, 1978).

1c. Cherniak (1990); 15-25% in Pappius (1982); >10% in Carpenter and Sutin (1983); 16-24% in Van Harreveld (1966).

1d. Cherniak (1990).

2. This figure is the sum of the figures derived below.

2a-b. We infer these in the following way: Sholl (1956) estimates that the surface area of the soma is 10% of the total neuronal surface, but Noback and Demarest (1975) suggest that this figure is only applicable to large neurons. We assume that the mean figure is 5%, while the dendrites take up 80% and the axon the remaining 15%. The figure for soma area is given in note *2d*. From these figures we calculate dendrite and axonal areas as 11200 and 2100 μm^2, respectively. We assume that the processes are regularly cylindrical and derive volumes and diameters.

2c. The standard neuron makes 10,000 outgoing synaptic connections and receives input from 10,000 synapses (c.f., Palm, 1982; Cherniak, 1990; Carpenter, 1984; Arbib, 1972). Each synapse has a diameter of 0.7 µm (Cragg, 1967), so its area is 0.4 μm^2, and its volume is 0.2 μm^3. Although only half the total synapse volume belongs to the standard neuron, to this must be added the volume of the unique pre-synaptic elements of the dendrites or axons. Cherniak (1990) suggests figures of 1-2 μm^3; we assume a figure of 0.6 μm^3 on each side of the synaptic cleft. This is a total of 6,000 μm^3. The 10,000 incoming synapses cover an area of 4,000 μm^2, which is 34% of the dendrite-plus-soma surface area.

2d. Cherniak (1990) estimates that cortical somata have a mean volume of 1,660 μm^3; he derives this figure from Blinkov and Glezer's (1968) calculations which give volumes from 297 μm^3 to 2,953 μm^3 for cortical pyramidals. (Also see, Sholl, 1956, for volumes for cat cortical somata of 550 - 19,620 μm^3). Assuming that the soma is a sphere allows the soma area and diameter to be calculated at 700μm^2 and 15µm respectively. The diameter estimate is within the range normally reported, e.g., 10-200 µm (Mitchell and Mayor, 1983), 6-100+ µm (Shepherd, 1974). Soma volume of cortex is 2.85% (Gerard in Weiss, 1950, quoting Bok), which is roughly 10% of total neuron volume (30%); this confirms the previous calculations which suggested that the soma forms 10% of the neuron volume.

3. All figures are derived by first calculating average neuron volume (neuron space volume, see *1b,* divided by number of neurons, see *4*), and than scaling each component by proportional reduction, using the percentage figures in *2.*

4. Dividing the neuron space, *1b,* by standard neuron volume, *2,* produces an initial estimate of 22 billion (10^9). This figure is clearly too low, because the standard neuron is much larger than the average neuron. Cerebellum contains 30 billion neurons (see Table 7), most of which are very small, and cortex contains 8.3 billion (see Table 5). Subtracting cerebellar and cortical volume from the whole brain volume, and repeating our first calculation produces a figure of 1.7 billion neurons to add to the cerebellar and cortical numbers. Our final estimate is larger than a range of previous estimates (all figures in billions): 10 (Carpenter, 1984; Arbib, 1972); 13 (Pfeiffer, 1955); 20 (Palm, 1982), but well below the often cited figure of 100 billion (e.g., Hubel, 1979; Stevens, 1979; Thompson, 1899; Sejnowski and Churchland, 1992).

5. Add *3a*, *3b,* and *3c,* and multiply by *4.*

6. Each standard neuron connects to about 10000 other neurons, see *2c,* but the average neuron makes about 2350 connections. This figure is the weighted average of 6.6 x 10^{13} cortical synapses (Table 5, note *6*), 1.7 x 10^{13} subcortical synapses, and 3 x 10^{12} cerebellar synapses, divided by the total number of neurons in the brain (note *4*).

7. Reported axon radii (including myelin sheaths) are 0.1-11 µm (Mitchell and Mayor, 1983), and 0.05-10 µm (Shepherd, 1974) in the human brain, and 0.15 µm in the mouse brain (Braitenberg and Schüz, 1991, p.43). Dendritic diameters are 0.05-7.5 µm (Shepherd, 1974) in humans and 0.45 µm in the mouse brain. Although the estimate we use is at the low end of the ranges quoted, it allows direct comparisons the figures derived by Nelson and Bower (1990).

Topology	Volume (m^3)	Synapses
Brain Connectivity Volume		
Unknown	0.000338	9.4×10^{13}
Interior Model		
Full	1780000	1.6×10^{21}
Random	0.105	9.4×10^{13}
k-Near	0.000223	4.0×10^{14}
Modular	0.00539	4.0×10^{14}
Exterior Cube Model		
Full	15300	1.6×10^{21}
Random	0.0578	9.4×10^{13}
k-Near	0.00000191	4.0×10^{14}
Modular	0.00544	4.0×10^{14}
Exterior Sphere Model		
Full	3102	1.6×10^{21}
Random	0.0117	9.4×10^{13}
k-Near	0.0000003877	4.0×10^{14}
Modular	0.00110	4.0×10^{14}

Table 4. Results for the homogeneous brain. Variables used are listed in Table 3. In addition, we have used the following estimates: $m = 100$, $b = 100$ (this gives $F = m/n = 2.5 \times 10^{-9}$), $x = 4.472 \times 10^{-6}$ (based on 50,000 neurons per mm^2), and $k = 10{,}000$ (see Table 3, note *2c*). All values have been rounded to three significant figures.

Notes	Variable	Value	Percentage
1	cortex volume	1035 cc	100%
1a	neocortex	1006.5 cc	97%
1b	grey matter	399 cc	38.5%
1c	white matter	607.5 cc	58.5%
1d	allocortex	28.5 cc	3%
1e	grey matter	14.3 cc	1.5%
1f	white matter	14.3 cc	1.5%
2	cortex surface area	165800 mm^2	100%
2a	neocortex	159600 mm^2	96.3%
2b	allocortex	6200 mm^2	3.7%
3	number of neurons per mm^2	50000	
4	number of neurons *(n)*	8.3×10^9	
4a	neocortical neurons	8.0×10^9	
4b	allocortical neurons	0.3×10^9	
5	total connection volume *(V=A)*	269.1 cc	
6	connectivity factor *(f)*	9.6×10^{-7}	

Table 5. Estimated values of the independent variables for the human cortex.

Notes to Table 5

1,a,d. Stephan et al (1970).

1b-c,e-f. Grey matter has an average thickness of 2.5 mm (Sholl, 1956; 3 mm in Eccles, 1981), and thus a volume of 414,500 mm^3. Other estimates are 230,000 in Shariff (1953), 548,000 in Sholl (1956) from Henneberg (1910), 572,000 in Sholl (1956) from Tramer (1916), 578,000 in Jaeger (1914), 580,000 in Sholl (1956) from Donaldson (1895). The remaining 620,500 mm^3 is white matter.

2. Jouandet *et al.* (1989); this agrees well with that of Blinkov and Glezer (1968); other estimates are 120,000 (Shepherd, 1974; Eccles, 1981), 139,000 (Hubel, 1979), 200,000 (Colonnier, 1981; Carpenter and Sutin, 1983), 218,800 (Henneberg, 1910), 229,000 (Tramer, 1916), 235,200 (Donaldson, 1895), 307,500 (Hofman, 1983).

2a-b. Neocortical surface area is from Jouandet et al (1990) and agrees with the often-stated assertion (e.g., Blinkov and Glezer, 1968) that neocortex is 95% of the total cortical area (96.3% to be exact); 2b = 2-2a.

3. Neurons per underlying mm^2 of surface area: Thompson (1899); 59,100 for Brodmann area 17, 44,300 for area 4 (Beaulieu and Colonnier, 1989), and 80,000 in Powell and Hendrickson (1981).

4. There are many ways to assess cortical neuronal population: neurons per unit volume, neurons per underlying unit area, and soma percentage of cortical tissue volume. Crick and Asanuma (1986) point out that the unit volume figures are much more variable than the underlying unit area figures (also see Braitenberg and Schüz, 1991, p.28). Using 50,000 neurons per underlying mm^2, yields a population estimate of 8.29 billion (10^9). This agrees well with that derived from the estimate that soma occupy 2.85% of cortical grey matter (Gerard in Weiss, 1950, quoting Bok), namely 7.12 billion.

For unit volume, 10,500 neurons per mm^3 is from Tower (1954) and Tower and Elliott (1952), 15,600 is from Cragg (1975), Cherniak (1990) uses 50,000 neurons per mm^3 as his estimate, and reports a range of estimates from 30,000 to 100,000 in e.g., Blinkov and Glezer (1968), Pope (1978), Peters (1987), O'Kusky and Colonnier (1982). Calculations based on 10,500 yield a total estimate of 4.4 billion neurons, while 50,000 yields 20.7 billion.

We assume that the surface area estimates are the most reliable, and that cortex has 8.3 billion neurons, of which 8 billion (i.e., 96.3%) are neocortical, and 0.3 billion are allocortical. This figure means that on average there are 20,000 neurons per mm^3 of cortical grey matter. Note that the population figure is within the range of previously published estimates, the mean of which is 7 billion: 1.2 billion (Donaldson, 1895), 5 billion (Agduhr,

1934), 6.25 billion (Sholl, 1956), 6.9 billion (Shariff, 1953), 9.3 billion (Thompson, 1899), 10 billion (Eccles, 1981), 14 billion (Economo and Koskinas, 1925).

5. Total connectivity volume in the cortex here represents 20% of grey matter space and 30% of white matter space. Non-neuronal space in the whole brain is 70% (see Table 3, note 1) in addition to which we must add the cell bodies in the grey matter contributing another 10% (see note 4), leaving 20% for axons, dendrites, etc. This extrapolation may be too low (cf. the estimate by Schüz and Palm, 1989, of 84% for mouse cortex), although it fits with Pope's (1988) estimate of 35-40% for neurons in human neocortex.

6. Based on an average of 8000 synapses per neuron and a total of 8.3 billion (10^9) neurons (see note *4*). This is the same number of synapses as found in the mouse cortex (Braitenberg and Schüz, 1991). Note that this is higher than some estimates, for example, 4000 (Cherniak, 1990) and 5000 (Douglas and Martin, 1991, excitatory synapses), but much lower than the observed figures of 15-30,000 (Colonnier, 1981) and 39,000 (Cragg, 1975). Our figure is based on the following calculation: with 20,000 neurons per mm^3 (see note *4*) there is a mean volume of 50,000 μm^3 available for each neuron; since 30% of this volume is actually occupied by neurons (see Table 3), each neuron has 15,000 μm^3 available; since each synapse occupies 0.6 μm^3 (Table 3, note *2.c*) and the they form 35% of the neuron (Table 3, note *2.c*), there cannot be more than 8750 synapses per neuron. We know of no strong evidence that the number of synapses per cortical neuron differs significantly between mammals, which is why we have rounded the latter figure down to 8000 so that it conforms to the figure of Braitenberg and Schüz (1991), which is based on a very thorough analysis. We can check these figures against Crick and Asanuma's (1986) approximations (see Table 9): the 3.2 billion stellates receive 300 ("a few hundred", p.338) synapses, the 2.9 billion small pyramids receive 3000 ("some thousands", p.338) and the 1.9 billion large pyramids receive 30,000 ("some tens of thousands", p.338). This is a total of 6.7×10^{13} synapses giving 8300 synapses per neuron (using a total of 8 billion neurons here). If each cortical neuron has 8,000 synapses there are 6.6×10^{13} cortical synapses, which is much lower than Colonnier's estimate (1981) of 3.0×10^{14} cortical synapses. Inhibitory synapses are 15% of the total; of the 85% excitatory synapses, 72% are to other excitatory neurons, and 13% are to the inhibitory neurons (Braitenberg and Schüz, 1991; Douglas and Martin, 1991).

3.2 The cerebral cortex

This section analyzes the quantitative details available for the cortex (Table 5). The results of our exploration of these figures are presented in Table 6. The first point to note is once again the enormous volumes generated by all of the fully connected topologies. Moving the neurons of an interior cube (or sphere) onto its surfaces reduces its total connectivity volume by nearly two orders of magnitude. Turning the cube into a sphere further reduces this connectivity volume by a factor five. The same general pattern repeats itself for the *k*-near topology, which once again generates very small connectivity overheads.

For both random and modular topologies the change from exterior cube to sphere similarly has the effect of a fivefold reduction in volume, but the change from interior to exterior cube affects these two topologies slightly differently. The random topology volume is more than halved, whereas the modular topology volume stays almost the same.

In terms of absolute numbers the modular exterior sphere topology is half the size of estimated size of the cortical connectivity volume, whereas the other two modular topologies are about twice as large. These are the only volume figures that come close to the empirical figure.

As a further demonstration of the plausibility of the modular structure we calculate that 350 modules (b = 50) exactly matches the connectivity volume of cortex, which compares favorably with Crick and Asanuma's (1986) recent estimate of 200 modules for neocortex, and Vogt and Vogt's (1919) early cytoarchitectonic estimate of 400 modules.

Topology	Volume (m^3)	Synapses
Cortical Connectivity Volume		
Unknown	0.000269	6.6×10^{13}
Interior Model		
Full	35000	6.9×10^{19}
Random	0.0336	6.6×10^{13}
k-Near	0.0000462	8.3×10^{13}
Modular	0.000574	8.3×10^{13}
Exterior Cube Model		
Full	444	6.9×10^{19}
Random	0.0136	6.6×10^{13}
k-Near	0.000000587	8.3×10^{13}
Modular	0.000519	8.3×10^{13}
Exterior Sphere Model		
Full	90.1	6.9×10^{19}
Random	0.00277	6.6×10^{13}
k-Near	0.000000119	8.3×10^{13}
Modular	0.000105	8.3×10^{13}

Table 6. Results for the cerebral cortex. Variables used are listed in Table 5. In addition, we have used the following estimates: $m = 100$, $b = 100$ (this gives $F = m/n = 1.21 \times 10^{-8}$), $x = 4.472 \times 10^{-6}$ (based on 50,000 neurons per mm^2), and $k = 10{,}000$ (see Table 3, note *2c*). All values have been rounded to three significant figures.

3.3 The Cerebellar cortex

As Shepherd (1974) says "the cerebellum has been a favorite subject for the geometricians and arithmeticians of the brain." (p.187) Table 7 presents the neuroanatomical data of the cerebellar cortex and Table 8 contains the results of fitting these to the expressions for the interior model and the exterior sphere. Since the seminal work of David Marr (1969) the structure of the cerebellum has been studied extensively. In our terminology we classify it as a *k*-near topology. As Table 8 shows, this topology is the only one that produces

volumes smaller than that observed. This is true for both interior and exterior models. The fitted volumes, however, are so small that soma volumes can no longer be discounted. In addition, the very large number of neurons would not fit at the surface of the small exterior sphere. We would have neuron densities of 13.5 billion (10^9) per mm^2, which gives an x value of 0.0086 µm. By comparison retinal rods have a peak density of 160,000 per mm^2 (Shepherd, 1974). One solution to this problem is the extensive folding which is observed for cerebellum. In this way, a considerable density can be reached indirectly. The resulting 'fractal' structure of the cerebellum lies somewhere between a pure exterior sphere and an interior model.

Notes	Variable	Value	Percentage
1	cerebellum volume	125 cc	100%
1a	hemispheres	112.5 cc	90%
1b	grey matter	38 cc	30.4%
1c	white matter	74.5 cc	59.6%
1d	deep structures	12.5 cc	10%
2	cortex surface area	40000 mm^2	
3	number of neurons *(n)*	30 x 10^9	
4	connection volume *(V=A)*	33.1 cc	
5	connectivity factor *(f)*	3.33 x 10^{-9}	

Table 7. Estimated values of the independent variables for the human cerebellar cortex.

Notes to Table 7

1. Stephan et al. (1970).

1.a-b Eccles et al. (1967).

2. Braitenberg and Atwood (1958); at a mean thickness of 950 µ.

3. Eccles (1977), divided into 30 billion (10^9) granules, 30 million Purkinjes, 200 million stellates. Shepherd (1974) suggests 40 billion granules, 14 million Purkinjes, 30 million stellates, and 1 million Golgis. A density of 2.4 million per mm^3 (Fox and Barnard, 1957), suggests that there is room for 48 billion granules. But simple calculations with the connectivity figures (see *5*) suggest that Eccles' (1977) figures are more self-consistent.

4. Calculations as for cerebral cortex.

5. Shepherd (1974) suggests that each Purkinje has 100,000-150,000 synapses from 80,000 granules and that each granule contacts 100-450 Purkinjes. Because the number of afferent synapses must equal the number of efferent synapses, we fix these numbers at 30 million Purkinje cells with 100,000 afferent synapses and 30 billion granule cells with 100 efferent synapses. This gives a total of roughly 3,000 billion synapses for about 30 billion cerebellar neurons, which gives the connectivity and nearest neighbor figures.

Topology	Volume (m^3)	Synapses
Cerebellar Connectivity Volume		
Unknown	0.0000331	3.0×10^{12}
Interior Model		
Full	868000	9.0×10^{20}
Random	0.00286	3.0×10^{12}
k-Near	0.000000167	3.0×10^{12}
Modular	0.00357	3.0×10^{14}
Exterior Sphere Model		
Full	1623	9.0×10^{19}
Random	0.000707	3.0×10^{12}
k-Near	3.13×10^{-10}	3.0×10^{12}
Modular	0.000719	3.0×10^{14}

Table 8. Results for the cerebellar cortex. Variables used are listed in Table 7. In addition, we have used the following estimates: m = 100, b = 100 and k = 100 (see Table 7, note *5*). All values have been rounded to three significant figures.

4. General discussion

We have shown that the exterior modular topology best fits the known neuroanatomical data for the whole brain and the cortex, when considered at a coarse-grained level of analysis. This does not, however, preclude the possibility that interior packing is found at smaller scales. We are able to derive precise bounds for the density below which interior models are more efficient than sheet models. These turn out to be relevant only at a microstructural level. The expressions for these bounds also predict that neuron density in grey matter is maximized by evolution subject to certain constraints. We use this finding as a possible explanation of the remarkable constancy of number of neurons per underlying mm^2 of cortex in all mammals and most parts of the cortex. At a mesostructural level, however, we find further evidence for the efficiency of sheeted (laminar) structures in reducing connectivity volume (cf. Mitchison, 1992). Finally, we consider the possibility that other topologies are good fits for the cortex in other species.

4.1 Cortical mesostructures: Quantitative neuroanatomy

To examine in more detail the structure of the neocortex we make three simplifying assumptions: *(i)* Neocortex has three layers (cf. Crick and Asanuma, 1986), Upper, Middle, and Deep. The layers correspond to the laminae of Brodmann (1909) in the following way: Upper comprises laminae II and III, Middle is lamina IV, Deep is laminae V and VI. *(ii)* Neocortex contains two broad categories of neurons, neurons with spines and neurons without spines (Crick and Asanuma, 1986; Braitenberg and Schüz, 1991). All spiny neurons are excitatory, all smooth neurons are inhibitory. Two types of spiny neuron are distinguished: pyramidals and spiny stellates. *(iii)* We assume that all projection neurons are pyramidals and that all the pyramidals are projection neurons (see for example Braitenberg, 1977; but also see Sholl, 1956, and Gilbert and Wiesel, 1981).

Layer	Excitatory cells	Billions	Inhibitory cells	Billions	Total
Cerebral cortex					
Upper	Pyramidals	2.9	Smooth Stellates	0.3	3.2
Middle	Spiny Stellates	1.6	-	-	1.6
Deep	Pyramidals	1.9	Smooth Stellates	1.3	3.2
Cerebellar cortex					
Upper	-	-	Stellates	0.2	0.2
Middle	-	-	Purkinje	0.03	0.03
Deep	Granules	30	Golgi	0.001	30.001

Table 9. Neuron types and their numbers in different layers of *(i)* cerebral and *(ii)* cerebellar cortex.

Notes to Table 9

(i) Upper and Deep layers contain roughly the same number of neurons, i.e., 3.2 billion (40%) (see e.g., Glees, 1973, for monkey figures). Neuron types have the following proportions: pyramidals 60% (4.8 billion), spiny stellates 20% (1.6 billion), smooth stellates 20% (1.6 billion) (Tömböl, 1974; also see Mitra, 1955, and Winfield *et al.*, 1980). Middle layer neurons are essentially all the small spiny stellates (Lund, 1973). *(ii)* The Upper (Molecular) layer is 400 µm thick (42%) and fills 16,000 mm^3; the Middle (Purkinje) layer is 50 µm thick (5%), and fills 2,000 mm^3; and the Deep (Granular) layer is 500 µm thick (53%), and fills 20,000 mm^3. The Upper layer contains Stellates, which are inhibitory on to Purkinjes in the Middle layer. The Deep layer contains Granules, whose parallel fibres contact Purkinje dendrites, and Golgis, which laterally inhibit the Granules.

From the figures in Table 9 we calculate that 4.8 billion (10^9) neurons project out of cortex (cf., 10 billion in Abeles', 1991, estimate). There are three types of projection, defined according to their targets: *(i)* commissural, to the opposite hemisphere; *(ii)* subcortical, to lower areas of the brain; *(iii)* association, to other areas of the same hemisphere. There are roughly 300 million commissural axons: 200 million in the corpus callosum (Eccles, 1981; Carpenter, 1984; c.f. 100 million in Abeles, 1991; 145 million in Nathan, 1987), and an estimated 50 million in each of the Anterior and Posterior Commissures. There are roughly 112 million subcortical projections, as follows: *(a)*

Thalamus: 50 million; *(b)* Striatum: 50 million; *(c)* Cerebellum: 5 million; *(d)* Spinal cord (Pyramidal tract): 2 million; *(e)* others: 5 million (all from Palm, 1982). This leaves 4.4 billion association projection neurons. These are either mid-range (1-10 mm, i.e., through the floor of each sulcus to connect adjacent gyri), or long-range (roughly 7 fasciculi). We know of no estimates of the sizes of the fasciculi; 20 million axons each seems a reasonable estimate. This accounts for 280 million axons (5.8%), and leaves 4.2 billion mid-range association axons (86.6%). These results deserve emphasis: the vast majority (i.e., 98.7%; cf., +99% in Abeles, 1991) of all projection neurons in the neocortex project to other cortical regions. A similar argument is put forward by Braitenberg and Schüz (1991) who refer to the cortex as an 'association machine'.

A refinement of this analysis makes this point even more strongly. Within any one area *(1)* the Upper layer projects to the Deep layer, *(2)* the Middle layer projects to the Upper layer and receives input from thalamus, and *(3)* the Deep layer projects subcortically. In terms of intracortical connections, *(1)* feedforward connections (i.e., from areas closer to the primary sensory areas) arise from the Upper layer and terminate in the Middle layer, while *(2)* feedback connections arise from both Upper and Deep layers and terminate in both Upper and Deep layers (Rockland and Pandya, 1979, Maunsell and Van Essen, 1983).

We calculate that if 50% of all intracortical projections are feedforward, and they all arise from the Upper layer, then this accounts for 2.2 billion of the Upper pyramidals. The remaining 0.7 billion Upper pyramidals, and 1.5 billion of the Deep pyramidals project back to other Upper and Deep layers. This means that the 1.6 billion small spiny stellates in the Middle layer are receiving input from 2.2 billion Upper layer pyramidals in addition to their input from 50 million thalamic axons. In other words, 99.9% of the neurons that input to the Middle layer are other cortical neurons. Note that this is not true of the primary sensory areas: from 5% (Garey and Powell, 1971) to 29% (Tigges and Tigges, 1979) of Middle layer synapses (in monkey striate cortex) are thalamocortical.

Table 9 also shows a similar analysis for the cerebellum to demonstrate that this type of structure is not limited to the cerebrum (see also retina, allocortex, and olfactory bulb for further examples of laminarity).

4.2 Cortical mesostructures: Analyses

We investigate packing strategies at a very small scale by comparing interior models with sheet models. We assume that these sheeted structures can be approximated by small areas of the exterior sphere model (see Table 2). We investigate at what parameter values the sheet model generates smaller volumes than the interior model:

$$V_{sheet} < V_{int} \qquad \textbf{(41)}$$

We call this value the critical density. For *k*-nearest neighbor, for example, we have

$$snxk < s^{\frac{3}{2}} nk^{\frac{3}{2}} \qquad \textbf{(42)}$$

or

$$k > s^{-1}x^2 \quad \textbf{(43)}$$

The resulting expressions for critical densities, above which laminar structures are more efficient, are as follows (modularity is not relevant at this local scale):

Full connectivity:

$$\hat{n} = \frac{x^2}{s} \quad \textbf{(44)}$$

Random connectivity:

$$\hat{fn} = \frac{x^2}{s} \quad \textbf{(45)}$$

k-Nearest neighbor connectivity:

$$\hat{k} = \frac{x^2}{s} \quad \textbf{(46)}$$

We have thus found that sheet models are more efficient if the critical density exceeds $x^2/s = \Theta = 637$ neurons, for cortical interneuron distance $x = 4.47 \times 10^{-6}$ m (based on 50,000 neurons per underlying mm^2, see Table 5, note *3*) and cross-sectional fibre surface area $s = \pi r^2 = 3.14 \times 10^{-14}$ m^2. This critical density Θ may be a constant of fundamental importance in the brain, since it emerges from all three topologies. Thus we predict that interior packing is used in 'microstructures' with local densities of less than 637 interconnected neurons.

At a mesostructural level, we predict the existence of sheeted structures in the cortex whenever the threshold of 637 connected neurons is exceeded. We know that cortex is very densely wired (e.g., Braitenberg and Schüz, 1991). We interpret both laminarisation and minicolumns (Hubel and Wiesel, 1972) as examples of horizontal and vertical sheeted structures. We infer that the density of local wiring exceeds the threshold of 637 neurons. We predict that within-laminar density, following an interior packing model, will fall below 637 neurons in general. A clear example of sheeted packing with high connection densities is the structure of the hippocampus where CA3 and the fascia dentata are dense sheets of neurons wrapped around each other with the connections running between them.

Mitchison (1991) also finds that in many cases it is advantageous to separate neurons and their connections. He presents a fine-grained analysis of stripes in the cortex arriving at the conclusion that combining two such areas would double the volume of the combined separate areas (i.e., four times the volume of one area). Our sheet expression (e.g., random topology) gives the same prediction. Suppose we have two small areas each with n_s neurons and with volume

$$V_s = \mathbb{X} n_s^2 f^{\frac{1}{2}} \tag{47}$$

Combining these two areas results in an area with $n_t = 2n_s$ neurons and a volume

$$V_t = \mathbb{X} n_t^2 f^{\frac{1}{2}} \tag{48}$$

$$= \mathbb{X} 4 n_s^2 f^{\frac{1}{2}} = 4 V_s \tag{49}$$

Here, it is assumed that f remains constant and thus that the number of synapses doubles. If we keep the total number of synapses constant by setting $f_t = f_s/2$, we have

$$V_t = \mathbb{X} 4 n_s^2 \left(\frac{f}{2}\right)^{\frac{1}{2}} = 2\sqrt{2} V_s \tag{50}$$

so that the combined volume increases only with the square root of the number of combined areas (also see Mitchison, 1992).

One of the most remarkable constancies in the brain is the number of neurons in the grey matter of cortex per underlying mm^2 (Beaulieu and Colonnier, 1989; Braitenberg and Schüz, 1991; Bok, 1959; Rockel et al., 1980; Thompson, 1899). Connectivity volume of sheets can only be reduced by minimizing cross-sectional area s or interneuron distance x (see Table 2). We postulate that both s and x have indeed been minimized by evolution. An important constraint on the minimization of s is conduction velocity. We take the constancy of neurons per underlying mm^2 as evidence that x has reached a minimum value. It is inefficient to increase the number of neurons per mm^2 grey matter, if their fibres cannot have full access to white matter. We, therefore, consider x to be the width of a single neuron's interface between gray and white matter, i.e., the cabling area for its afferent and efferent fibres. As we have derived above, each neuron in the grey-matter layer will have connections to at least 637 (i.e., x^2/s) other neurons on average. From the above result we conclude that this interface must have room for at least 637 fibres per neuron and that this number sets the lower limit on x.

Further evidence for this conjecture is that the only area where the number of neurons per underlying mm^2 is much higher, area 17, has the most noticeable laminar structure with the Stria Gennarii representing a layer of white matter within the grey matter of that area (cf. Mitchison, 1992).

4.3 Brain size and equipotentiality

One of our main conclusions is that for the human brain, fully random topologies are not feasible. Even with very low connectivity factors the predicted volumes exceed the empirical values many times. We have also fit some of our volume expressions to the data for the mouse cortex which is about a thousand times smaller than the human cortex.

Braitenberg and Schüz (1991) arrive at the following estimates for a single hemisphere of the mouse cortex (including the hippocampus): $n = 8 \times 10^6$, $V = 90$ mm^3 (p.30) and the average number of synapses per neuron is 7826 which gives $f = 7826/n = 0.000978$. Compared with the human cortex the mouse brain is thus connected very densely: its connectivity factor is more than a thousand times higher. To investigate the effect of high connectivity with fewer neurons and lower volume, we have plotted the number of synapses as a function of the number of neurons in Figure 3, using random topologies. Figure 3.a uses the human data for the cortex as given in Table 5 (with $n = 4.15 \times 10^9$ and $V = A = 134.5$ cc, i.e., half the values given in the table). Figure 3.c is based on the figures cited above. The volume for a single hemisphere must be corrected for the presence of neuron bodies, blood vessels, etc.. Using the figures given in Braitenberg and Schüz (1991, p.43) we arrive at $V = 90 \times 0.442 = 39.8$ mm^3 as the connectivity volume for a single hemisphere. We have assumed that half of the post-synaptic neurons of any given neuron are distributed randomly throughout the same cortical hemisphere. The contribution of transcallosal fibers is ignored in these analyses.

As we can see in Figure 3.a, the predicted number of synapses for human cortex is much lower than the observed number of synapses (566 compared with 4000, i.e., 8000/2). Because callosal fibers have been ignored the figure of 566 synapses can be considered a high estimate. If we compare this estimate with that for the mouse in Figure 3.c, we find that the predicted value, 2822, approaches the observed value of 3913 synapses much more closely.

We conclude from this that whereas a fully random topology is very implausible for the human cortex, it is feasible for the mouse cortex. The human cortex must rely more heavily on other topologies such as modular and nearest neighbor. If this conclusion is correct, it would explain why the mouse and rat cortices have been shown to exhibit a high degree of equipotentiality and distributed memory representations (Lashley, 1950), whereas in humans and primates a much more modular and localized pattern is consistently observed (Shallice, 1988). Broadly similar conclusions are reached by Ringo (1991) and Hofman (1985) based on different formalisms. The mouse cortex can ’afford’ to be largely randomly connected with a high density, in this way approaching what Braitenberg and Schüz (1991) have called the ’mixing machine’.

An important further observation is that for the parameter ranges studied here the interior physical model performs much worse than the exterior sphere model. In Figure 3.b we have repeated the same plot as Figure 3.a, but now using the interior model. As soon as the number of neurons exceeds 100 million the predicted number of random synapses falls below 1. For the mouse cortex, the interior model still performs much worse than the exterior model as can be seen in Figure 3.d.

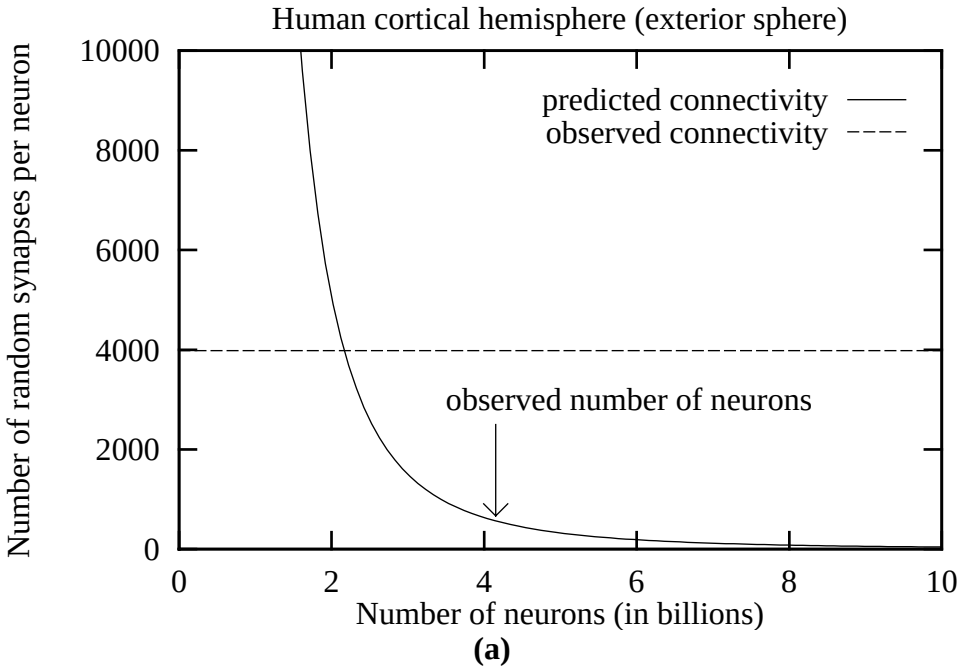

(a)

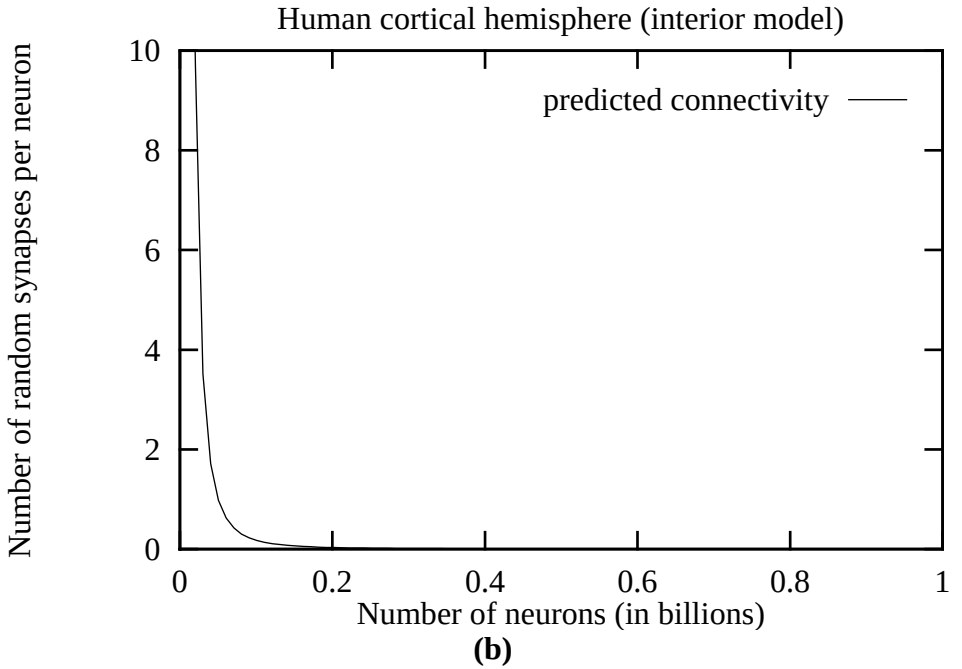

(b)

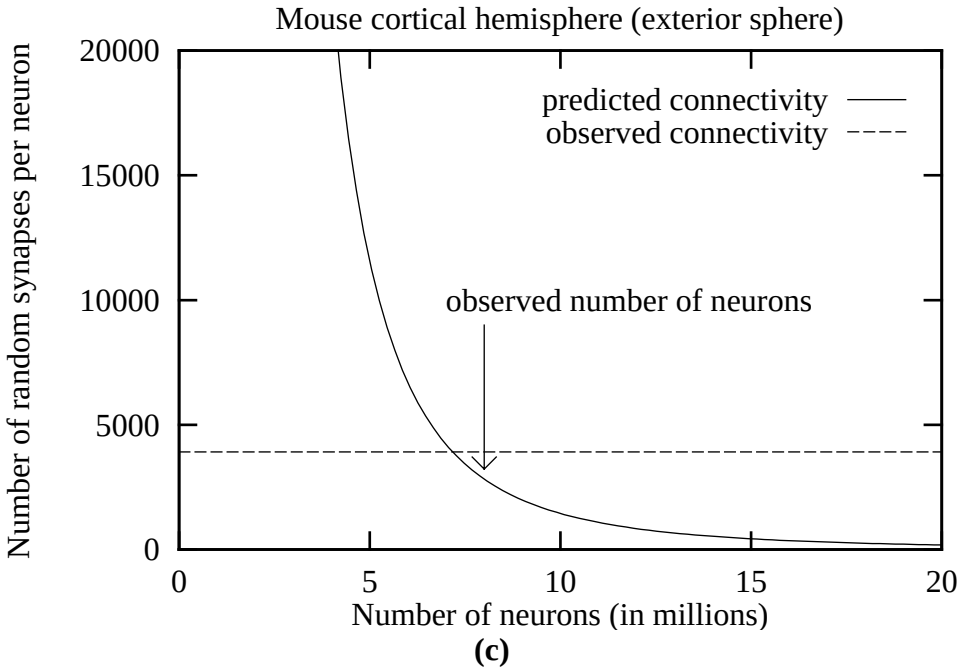

(c)

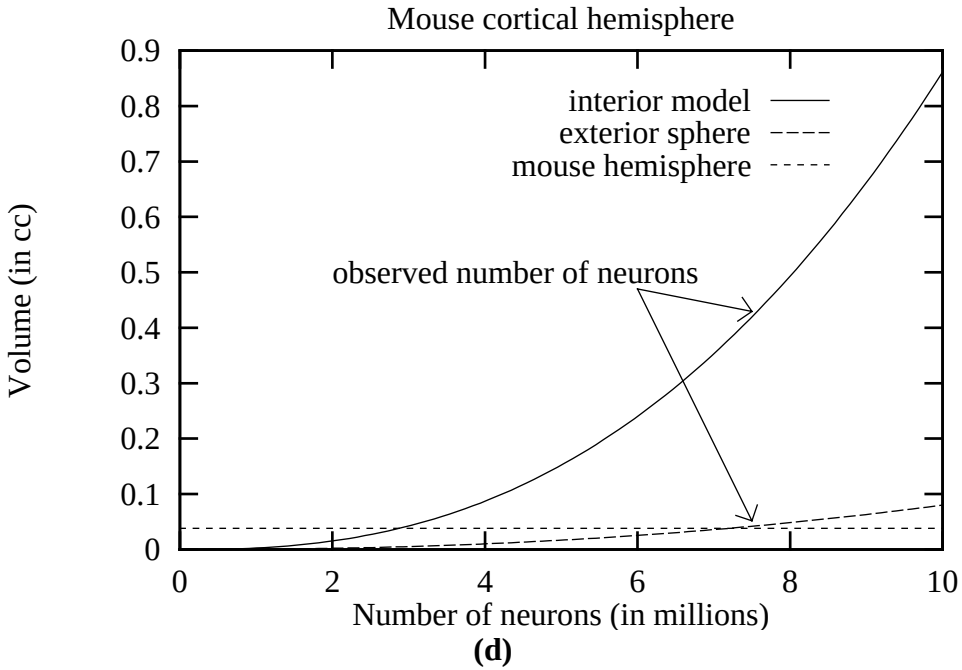

(d)

Figure 3. Random topologies in single cortical hemispheres in humans (a-b) and in the mouse (c-d). See text for further explanation. The parameters used are $r = 1.0 \times 10^{-7}$ (or $s = 3.14 \times 10^{-14}$) and $x = 4.472 \times 10^{-6}$.

4.4 Some functional implications of topologies

Our analyses are solely concerned with the structure of connectivity and completely disregard functional aspects. Nevertheless, we can make some conjectural inferences about the functioning of cerebellar and cerebral cortex. We assume that episodic memory representations require as random a topology as possible, given the unconstrained character of the contents of episodes. A *k*-near topology as found in the cerebellum would not suffice for extensive storage of episodes, specialized as it is for processing highly contiguous data.

We have shown that mouse cortex is better described as a random topology than human cortex, although even for mouse cortex there is good evidence for modularity (Braitenberg and Schüz, 1991). A mixture of random and modular topologies can be interpreted as supporting a view of cortex as both broadly delimiting what can be learned efficiently and allowing all specific experiences within those limits to be learned.

Since human cortex is sparsely wired, episodic memory is faced with a connectivity problem in that it involves associations between random sites in the cortex. As we have shown in this paper, the probability of direct connections between such sites is extremely small. Such associations can be established indirectly (Abeles, 1991) but this takes more time than the one-shot learning typical of episodic memory. A possible solution to this problem is the largely hierarchical macrostructure of the cortex, with the hippocampal area functioning as a temporary scaffold connecting distant sites in the cortex. A connectionist model of this has been developed by us, which is also able to explain characteristics and recovery patterns of anterograde amnesia, retrograde amnesia, and semantic dementia (Murre, submitted).

5. Concluding remarks

The human brain contains ten million kilometers of wiring (338 cc/3.14 x 10^{-14} m; cf. the Churchland and Sejnowski, 1992, figure of 100,000 km). In this paper we have looked at the various ways in which this very considerable length of fibers can be organized. We have developed a mathematical formalism for calculating connectivity volumes generated by specific topologies with various physical packing strategies. By extensive cross-referencing of available human neuroanatomical data we have produced a consistent set of parameters for the whole brain, the cerebral cortex, and the cerebellar cortex.

By comparing these inferred values with those predicted by the expressions, we were able to draw the following general conclusions for the human brain, cortex, and cerebellum: *(i)* Interior packing is less efficient than exterior packing (in a sphere). *(ii)* Fully and randomly connected topologies are extremely inefficient.

More specifically we found evidence that different topologies and physical packing strategies might be used at different scales. *(iii)* For the human brain at a macrostructural level, modular topologies on an exterior sphere approach the data most closely. *(iv)* On a mesostructural level, laminarization and columnarization are evidence of the superior efficiency of organizing the wiring as sheets. *(v)* Within sheets, microstructures emerge in which interior models were shown to be the most efficient.

With regard to interspecies similarities and differences we conjectured *(vi)* that the remarkable constancy of number of neurons per underlying mm^2 of cortex may be the result of evolution minimizing the *x* parameter in our expressions for the sheet, and *(vii)* that the topologies that best fit the human brain should not be assumed to apply to other mammals, such as the mouse.

We emphasize that these conclusions are preliminary, based as they are on an incomplete database and simplified models of the brain. Our identification of the mesostructural level of the brain is intended to mark a need for more accurate quantitative data. These are becoming increasingly important for connectionist models of human and animal functioning as they gain in size and plausibility. Our expressions can be refined in several ways, for example, by using axons that decrease in area with distance, by distinguishing short-range and long-range connections with different radii, and by using gradients of connectivity (e.g., Gaussian distributions; their effect would be intermediate between *k*-near and random topologies).

As pointed out by Mitchison (personal communication) connectivity from the axons to the soma (i.e., the dendrites) may in certain cases alter the above results. Preliminary analyses by ourselves suggest that in most cases the contribution of the dendrites can be expressed as a constant proportion of total connectivity volume. Thus, for connectivity volumes derived above we might add a proportion to account for dendritic volume, but at this point we are able to predict this contribution for only a subset of the above models. Other extensions might take into account such constant volumes as soma, blood vessels, and glia, as well as specific volume shapes such as hollow ellipsoids, all of which might have different effects on the models and topologies above. We do not believe that such refinements will alter our conclusions significantly, but they are an important next step in the application of the model. We are currently also applying our expressions to the available data for other animal species.

References

Ackley, D.H., Hinton, G.E., & Sejnowski, T.J. (1985). A learning algorithm for Boltzmann machines. *Cognitive Science*, 9, 147-169.

Abeles, M. (1991). *Corticonics: Neural circuits of the cerebral cortex*. Cambridge: Cambridge University Press.

Agduhr, E. (1934). Vergleich der Neuritenanzahl in dem Wurzeln der Spinalnerven bei Kröte, Maus, Hund und Mensch. *Z. Anat.*, 102, 194-210.

Anderson, J.A. (1972). A simple neural network generating an interactive memory. *Mathematical Biosciences*, 14, 197-220.

Anninos, P.A., Beek, B., Csermely, T.J., Harth, E.M., & Pertile, G. (1970). Dynamics of neural structures. *Journal of Theoretical Biology*, 26, 121-148.

Arbib, M.A. (1972). *The metaphorical brain: an introduction to cybernetics as artificial intelligence and brain theory*. New York: Wiley.

Beaulieu, C., & Colonnier, M. (1989). *Journal of Comparative Neurology*, 279, 228-234.

Blinkov, S., & Glezer, I. (1968). *The human brain in figures and tables: a quantitative handbook*. New York: Plenum Press.

Bok, S.T. (1959). *Histonomy of the cerebral cortex.* Amsterdam: Elsevier.

Braitenberg, V., & Atwood, R.P. (1958). Morphological observations on the cerebellar cortex. *Journal of Comparative Neurology,* 109, 1-33.

Braitenberg, V. (1977). *On the texture of brains.* Berlin, Heidelberg, New York: Springer-Verlag.

Braitenberg, V., & Schüz, A. (1991). *Anatomy of the cortex: statistics and geometry.* Berlin: Springer-Verlag.

Brodmann, K. (1909). *Vergleichende Lokalisationslehre der Grosshirnrinde.* [Principles of comparative localization in the cerebral cortex presented on the basis of cytoarchitecture]. Leipzig: Barth.

Carpenter, M., & Sutin, J. (1983). *Human neuroanatomy* (8th ed.). Baltimore: Williams & Wilkins.

Carpenter, R.H.S. (1984). *Neurophysiology.* London: Edward Arnold.

Cherniak, C. (1990). The bounded brain: toward quantitative neuroanatomy. *Journal of Cognitive Neuroscience,* 2, 58-68.

Cherniak, C. (1994). Component placement optimization in the brain. *Journal of Neuroscience,* 14, 2418-2427.

Colonnier, M.L. (1981). The electron-microscopic analysis of the neuronal organization of the cerebral cortex. In: Schmitt, F., Worden, F., Adelman, G., & Dennis, S. (Eds.), *The organization of the cerebral cortex.* Cambridge, MA: MIT Press.

Cragg, B. (1967). The density of synapses and neurons in the motor and visual areas of the cerebral cortex. *Journal of Anatomy,* 101, 639-654.

Cragg, B. (1975). The density of synapses and neurons in normal, mentally defective and ageing human brains. *Brain,* 98, 81-90.

Crick, F.H.C., & Asanuma, C. (1986). Certain aspects of the anatomy and physiology of the cerebral cortex. In: McClelland, J.L., & Rumelhart, D.E. (Eds.), *Parallel distributed processing: explorations in the microstructure of cognition, vol. 2. psychological and biological models.* Cambridge, MA: MIT Press.

Derrida, B., Gardner, E., & Zippelius, A. (1987). An exactly solvable asymmetric neural network model. *Europhysics Letters,* 4, 167-173.

Donaldson, H.H. (1895). *The growth of the brain.* Chicago.

Douglas, R.J., & Martin, K.A.C. (1991). Opening the grey box. *Trends in Neurosciences,* 14, 286-293.

Eccles, J.C. (1977). An instruction-selection theory of learning in the cerebellar cortex. *Brain Research,* 127, 327-352.

Eccles, J.C. (1981). The modular operation of the cerebral neocortex considered as a material basis for mental events. *Neuroscience,* 6, 1839-1856.

Eccles, J.C., Ito, M., & Szentagothai, J. (1967). *The cerebellum as a neuronal machine.* Springer-Verlag, Berlin, Heidelberg, New York.

Economo, C. Von, & Koskinas, G.N. (1925). *Die cytoarchitek-cerebral cortex*. Oxford.

Felleman, D.J., & Van Essen, D.C. (1991). *Distributed hierarchical processing in the primate cerebral cortex.* Cerebral Cortex, 1, 1-47.

Fox, C.A., & Barnard, J.W. (1957). A quantitative study of the Purkinje cell dendritic branchlets and their relationship to afferent fibers. *Journal of Anatomy,* 91, 299-313.

Garey, L.J., & Powell, T.P.S. (1971). An experimental study of the termination of the lateral geniculo-cortical pathway in the cat and monkey. *Proceedings of the Royal Society of London, Series B,* 179, 41-63.

Gilbert, C.D., & Wiesel, T.M. (1981). Laminar specialization and intracortical connections in cat primary visual cortex. F.O. Schmitt et al (eds.), *The Organization of the Cerebral Cortex*, MIT Press.

Glees, P. (1973). The neuroglial compartments at light microscopic and electron microscopic levels. In: Balazs R., & Cremer, J.E. (Eds.), *Metabolic Compartmentation in the Brain*. London & Basingstoke: Macmillan.

Grossberg, S. (1976). Adaptive pattern classification and universal recoding, II: Feedback, expectation, olfaction, and illusions. *Biological Cybernetics*, 23, 187-202.

Grossberg, S. (1982). *Studies of mind and brain: neural principles of learning, perception, development, cognition, and motor control*. Boston: Reidel Press.

Grossberg, S. (1987). *The adaptive brain. Volume I: Cognition, learning, reinforcement, and rhythm. Volume II: Vision, speech, language, and motor control*. Amsterdam: North-Holland.

Harth, E.M., Csermly, T.J., Beek, B., & Lindsay, R.D. (1970). Brain function and neural dynamics. *Journal of Theoretical Biology*, 26, 93-120.

Henneberg, R. (1910). Messung der Oberflächenausdehnung der Grosshirnrinde. [Measurement of the surface area of the cerebral cortex]. *Journal für Psychologie und Neurologie* (Leipzig), 17, 144-158.

Hofman, M.A. (1985). Neuronal correlates of corticalization in mammals: a theory. *Journal of Theoretical Biology*, 112, 77-95.

Hopfield, J.J. (1982). Neural networks and physical systems with emergent collective computational abilities. *Proceedings of the National Academy of Sciences, USA*, 79, 2554-2558.

Hopfield, J.J. (1984). Neurons with graded response have collective computational properties like those of two-state neurons. *Proceedings of the National Academy of Sciences*, 71, 3088-3092.

Hubel, D.H., & Wiesel, T.N. (1972). Laminar and columnar distribution of geniculo-cortical fibres in the Macaque monkey. *Journal of Comparative Neurology*, 146, 421-450.

Hubel, D.H. (1979). The brain. *Scientific American*, 241, 38-47.

Jaeger, R. (1914). Inhaltsberechnungen der Rinden und Marksubstanz des Grosshirns durch planimetrische Messungen. *Arch. Psychiat.*, 54, 261-272.

Jouandet, M., Tramo, M., Herron, D., Hermann, A., Loftus, W., Bazell, J., & Gazzaniga, M. (1989). Brainprints: computer-generated two-dimensional maps of the human cerebral cortex in vivo. *Journal of Cognitive Neuroscience*, 1, 88-117.

Kohonen, T. (1972). Correlation matrix memories. *IEEE Transactions on Computers*, C-21, 353-359.

Kohonen, T. (1989). *Self-organization and associative memory*, 3rd edition, Berlin Germany: Springer-Verlag.

Kohonen, T. (1990). The self-organizing map. *Proceedings of the IEEE*, 78, 1464-1480.

Kosko, B. (1987). Adaptive bidirectional associative memories. *Applied Optics*, 26, 4947-4960.

Kosko, B. (1988). Bidirectional associative memories. *IEEE Transactions on Systems, Man, and Cybernetics*, SMC-18, 49-60.

Lashley, K.S. (1950). In search of the engram. *Society of Experimental Biology Symposium, No.4: Psychological Mechanisms in Animal Behavior*. Cambridge: Cambridge University Press, 454-480.

Lorente de No, R. (1938). Cerebral cortex: architecture, intracortical connections, motor projections. In: Fulton, J.F. (Ed.), *Physiology of the Nervous System*. New York: Oxford University Press.

Lund, J.S. (1973). Organization of neurons in the visual cortex, Area 17, of the monkey (Macaca mulatta). *Journal of Comparative Neurology*, 147, 455-496.

Marr, D. (1969). A theory of cerebellar cortex. *Journal of Physiology (London)*, 202, 437-470.

Maunsell, J.H.R., & Van Essen, D.C. (1983). The connections of the middle temporal visual area (MT) and their relation to a cortical hierarchy in the macaque monkey. *Journal of Neuroscience*, 3, 2563-2586.

Mesulam, M.M., Murson, E.J., Levely, A., & Wainer, B.H. (1983). Cholinergic innervation of cortex by the basal forebrain: cytochemistry and cortical connections of the septal area, diagonal band nuclei, nucleus basalis (substantia innominata), and hypothalamus in the rhesus monkey. *Journal of Comparative Neurology*, 214, 170-197.

Mitchell, G.A.G., & Mayor, D. (1983). *The essentials of neuroanatomy*, Fourth Edition. Churchill Livingstone.

Mitchison, G.J. (1991). Neuronal branching patterns and the economy of cortical wiring. *Proceedings of the Royal Society, London, B*, 245, 151-158.

Mitchison, G.J. (1992). Axonal trees and cortical architecture. *Trends in Neurosciences*, 15, 122-126.

Mitra, N.L. (1955). A quantitative analyses of cell types in mammalian neo-cortex. *Journal of Anatomy (London)*, 89, 467-483.

Mountcastle, V.B. (1978). An organizing principle for cerebral function: the unit module and the distributed system. In: Edelman G.M., & Mountcastle, V.B. (Eds.) *The mindful brain*. Cambridge, MA: MIT Press.

Murre, J.M.J. (1992). *Categorization and learning in modular neural networks*. Hemel Hempstead: Harvester Wheatsheaf. Co-published by Lawrence Erlbaum in the USA and Canada (Hillsdale, NJ).

Murre, J.M.J. (1993). Transputers and neural networks: an analysis of implementation constraints and performance. *IEEE Transactions on Neural Networks*, 4, 284-292.

Murre, J.M.J. (submitted). *A model of amnesia.* Submitted to Psychological Review.

Nakano, N. (1972). Associatron: a model of associative memory. *IEEE Transactions on Systems, Man, and Cybernetics.* SMC-2, 381-388.

Nathan, P.W. (1987). Nervous System. In: Gregory, R.L. (Ed.), *The Oxford companion to the mind*. Oxford: Oxford University Press.

Nelken, I. (1988). Analysis of the activity of single neurons in stochastic settings. *Biological Cybernetics*, 59, 201-215.

Nelson, M.E., & Bower, J.M. (1990). Brain maps and parallel computers. *Trends in Neurosciences*, 13, 403-408.

Noback, C.R., & Demarest, R.J. (1975). *The human nervous system* (2nd ed.). New York: McGraw-Hill.

O'Kusky, J., & Colonnier, M. (1982). A laminar analysis of the number of neurons, glia and synapses in the visual cortex (area 17) of adult macaque monkeys. *Journal of Comparative Neurology*, 210, 278-290.

Palm. G. (1982). *Neural assemblies: an alternative approach to artificial intelligence*. Berlin, Heidelberg, New York: Springer-Verlag.

Pappius, H. (1982). Water spaces. In: Lajtha, A. (Ed.), *Handbook of neurochemistry* (Vol. 1, 2nd ed.). New York: Plenum.

Peters, A. (1987). Number of neurons and synapses in primary visual cortex. In: Jones, E., & Peters, A. (Eds.), *Cerebral Cortex (Vol. 6)*. New York: Plenum.

Pfeiffer, J. (1955). *The human brain*. London: Victor Gollancz Ltd.

Pope, A. (1978). *Neuroglia: quantitative aspects.* In: Schoffeniels, E., Franck, G., Hertz, L., & Tower, D. (Eds.), Dynamic properties of glia cells. New York: Pergamon.

Powell, T.P.S., & Hendrickson, A.E. (1981). Similarity in number of neurons through the depth of the cortex in the binocular and monocular parts of area 17 of the monkey. *Brain Research*, 216, 409-413.

Ringo, J.L. (1991). Neuronal interconnection as a function of brain size. *Brain, Behavior, and Evolution*, 38, 1-6.

Rockel, A.J., Hiorns, R.W., & Powell, T.P.S. (1980). The basic uniformity in structure of the neocortex. *Brain*, 103, 221-244.

Rockland, K.S., & Pandya, D.N. (1979). Laminar origins and terminations of cortical connections of the occipital lobe in the rhesus monkey. *Brain Research*, 179, 3-20.

Rolls, E.T. (1990). Functions of neuronal networks in the hippocampus and of backprojections in the cerebral cortex in memory. In: McGaugh, J.L., Weinberger, N.M., & Lynch, G. (Eds.), *Brain organization and memory: cells, systems, and circuits.* Oxford: Oxford University Press.

Rumelhart, D.E., Hinton, G.E., & Williams, R.J. (1986). Learning internal representations by error propagation. In: Rumelhart, D.E., & McClelland, J.L. (Eds.), *Parallel distributed processing. Volume 1.* Cambridge, MA: MIT Press, 318-362.

Schüz, A., & Palm, G. (1989). Density of neurons and synapses in the cerebral cortex of the mouse. *Journal of Comparative Neurology*, 286, 442-455.

Seifert, W. (Ed.) (1984). *Neurobiology of the hippocampus*. London: Academic Press.

Sejnowski, T.J., & Churchland, P.S. (1992). Silicon brains. *Byte*, 137-146.

Shallice, T. (1988). *From neuropsychology to mental structure*. Cambridge: University Press.

Shariff, G.A. (1953). Cell counts in the primate cerebral cortex. *Journal of Comparative Neurology*, 98, 381-400.

Shepherd, G. (1974). *The synaptic organization of the brain.* New York: Oxford University Press.

Shinomoto, S. (1987). A cognitive and associative memory. *Biological Cybernetics*, 57, 197-206.

Sholl, D.A. (1956). *The organization of the cerebral cortex.* Methuen, London.

Steinbuch, K. (1961). Die Lernmatrix. *Kybernetik*, 1, 36-45.

Stephan, H., Bauchot, R., & Andy, O.J. (1970). Data on size of the brain and of various brain parts in insectivores and primates. In: Noback, C.R., & Montagna, W. (Eds.), *The primate brain*. New York: Appleton-Century-Crofts, 289-297.

Stevens, C.F. (1979). The neuron. *Scientific American*, 241, 48-59.

Szentágothai, J. (1975). The 'module-concept' in cerebral cortex architecture. *Brain Research*, *95*, 475-496.

Thompson, H. (1899). The total number of functional nerve cells in the cerebral cortex of man. *J. Comp. Neurol.*, 9, 113-140.

Tigges, M., & Tigges, J. (1979). Types of degenerating geniculocortical axon terminals and their contribution to layer IV of area 17 in the squirrel monkey (Saimiri). *Cell and Tissue Research*, 196, 471-486.

Tömböl, T. (1974). An electron microscopic study of the neurons of the visual cortex. *Journal of Neurocytology*, 3, 525-531.

Tower, D.B., & Elliott, K.A.C. (1952). Activity of the acetylcholine system in cerebral cortex of various unanesthetized animals. *Am. J. Physiol.*, 168, 747-759.

Tower, D.B. (1954). Structural and functional organization of mammalian cerebral cortex: The correlation of neurone density with brain size. *J. Comp. Neurol.*, 101, 19-52.

Tramer, M. (1916). Über Messung und Entwicklung der Rindenoberfläche des menschlichen Grosshirns. *Arb. Hirnanat.* Inst., Zurich, 10, 5-57.

Treves, A., &, E.T. Rolls (1994). Computational analysis of the role of the hippocampus in memory. *Hippocampus*, 4, 374-391.

Van Harreveld, A. (1966). In: Cavaness W.F., & Walker, A.E. (Eds.), *Head Injury, Conference Proceedings.* Philadelphia & Toronto: Lippincott.

Weiss, P. (Ed.) (1950). *Genetic neurology.* University of Chicago Press.

Vernadakis, A. (1986). Changes in astrocytes with aging. In: Fedoroff S., & Vernadakis, A. (Eds.), *Astrocytes: biochemistry, physiology, and pharmacology of astrocytes (Vol. 2)*. Orlando, Fla.: Academic Press.

White, E.L. (1989). *Cortical circuits: synaptic organization of the cerebral cortex: structure, function, and theory.* Boston, MA: Birkhäuser.

Winfield, D.A., Gatter, K.L., & Powell, T.P.S. (1980). An electron microscope study of types and proportions of neurons in the cortex of the motor and visual areas of the cat and rat. *Brain*, 103, 245.